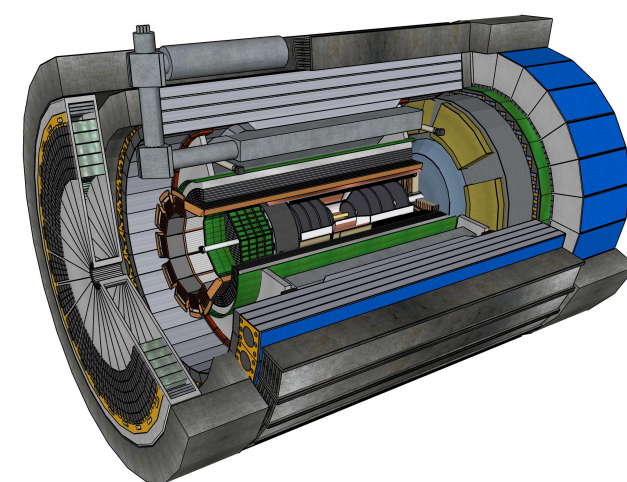
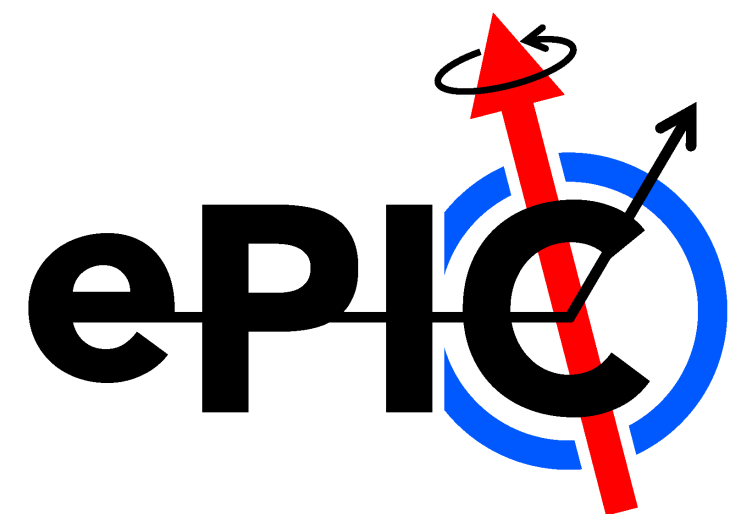


# ePIC/EIC resolutions and systematics

Tyler Kutz (MIT)

INT-24-87W: Electroweak and  
Beyond the Standard Model Physics at the EIC

February 12, 2024

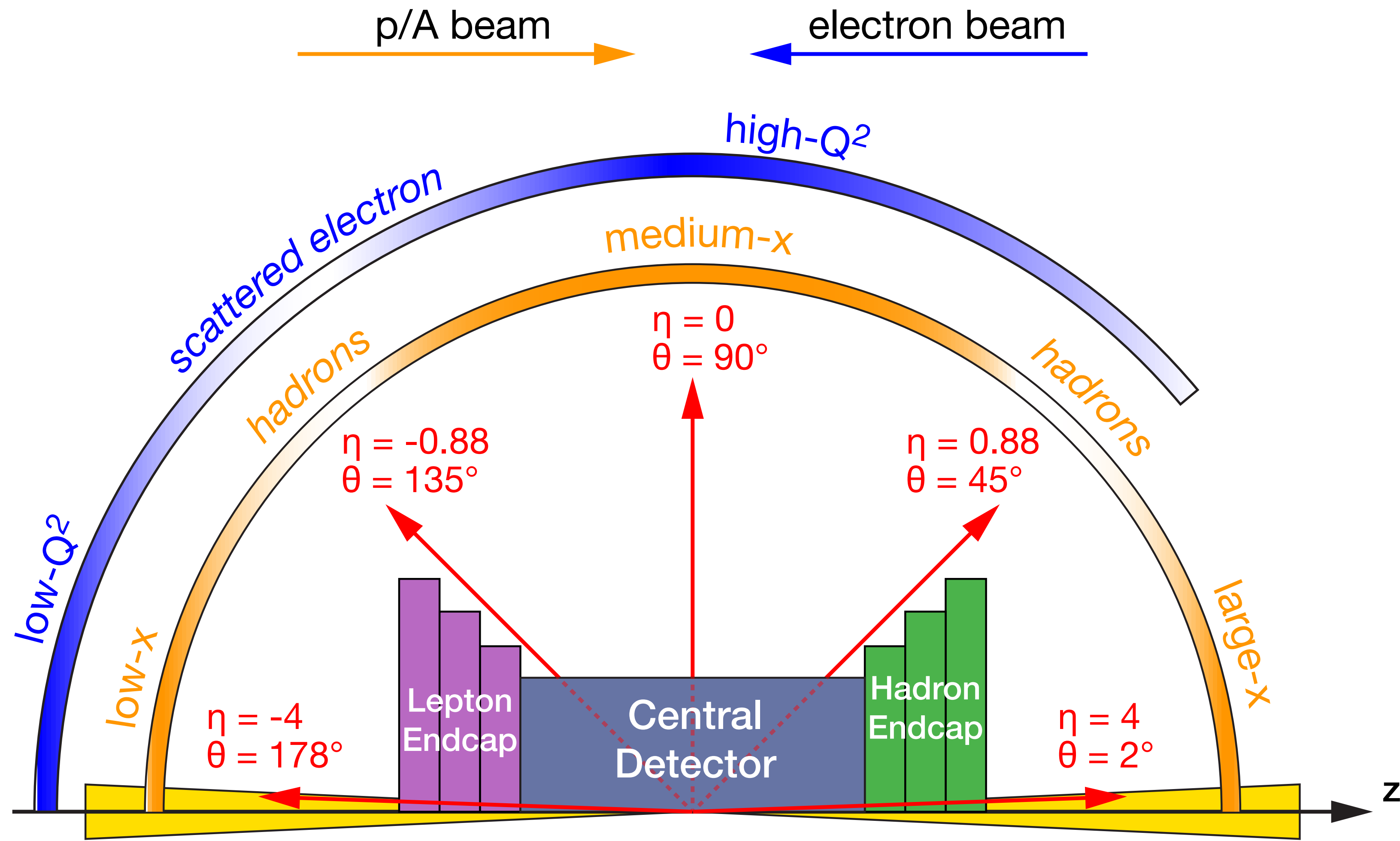


# Two caveats

It's difficult to evaluate systematics for an experiment 10 years in the future.

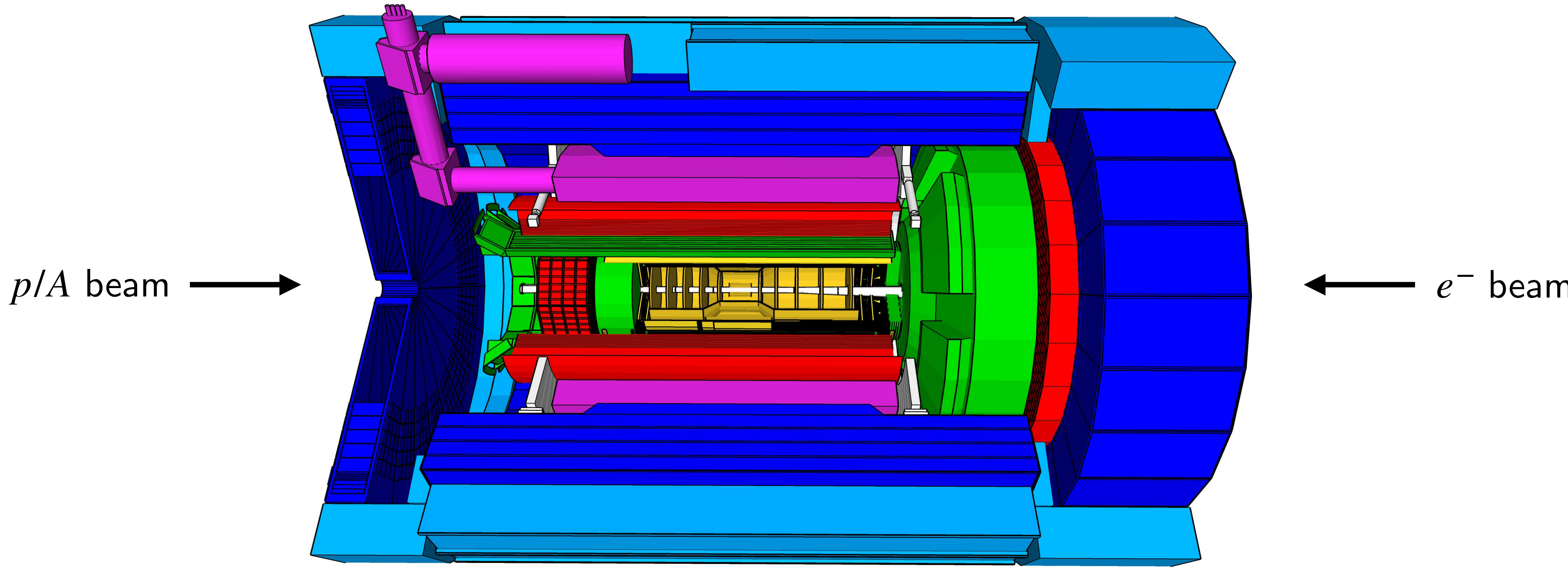
Current simulations/reconstruction results subject to improvement!

# ePIC designed to be hermetic, multi-purpose detector

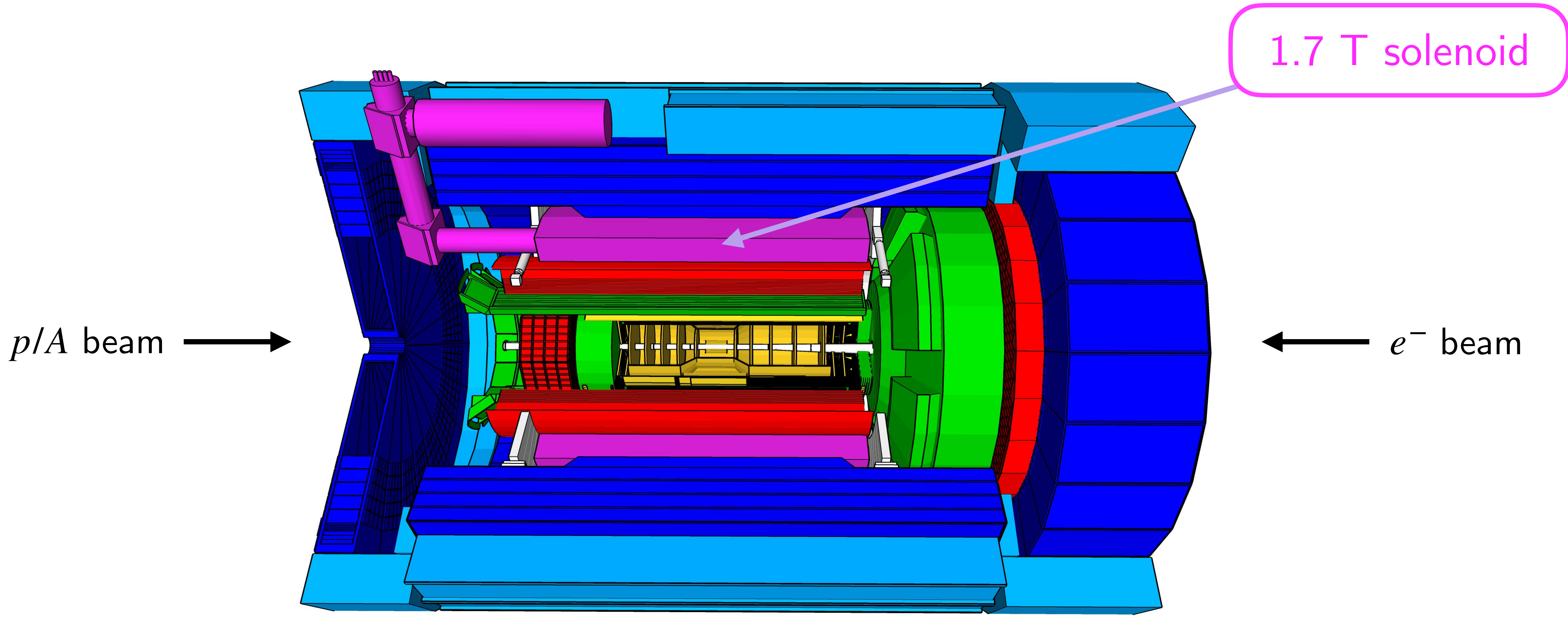


Reconstruction of *both* scattered electron *and* hadronic final state critical to EIC physics program

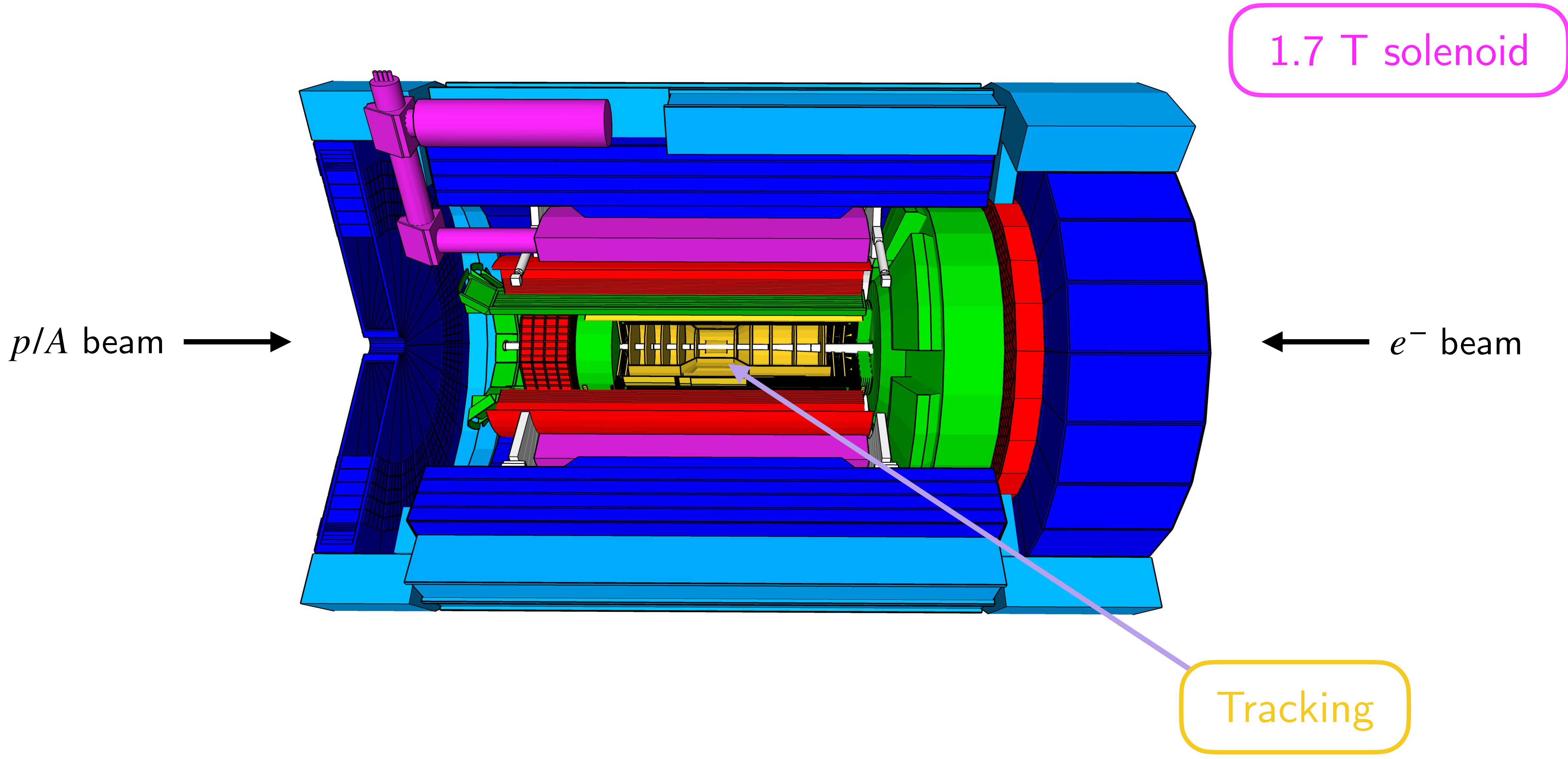
# ePIC designed to be hermetic, multi-purpose detector



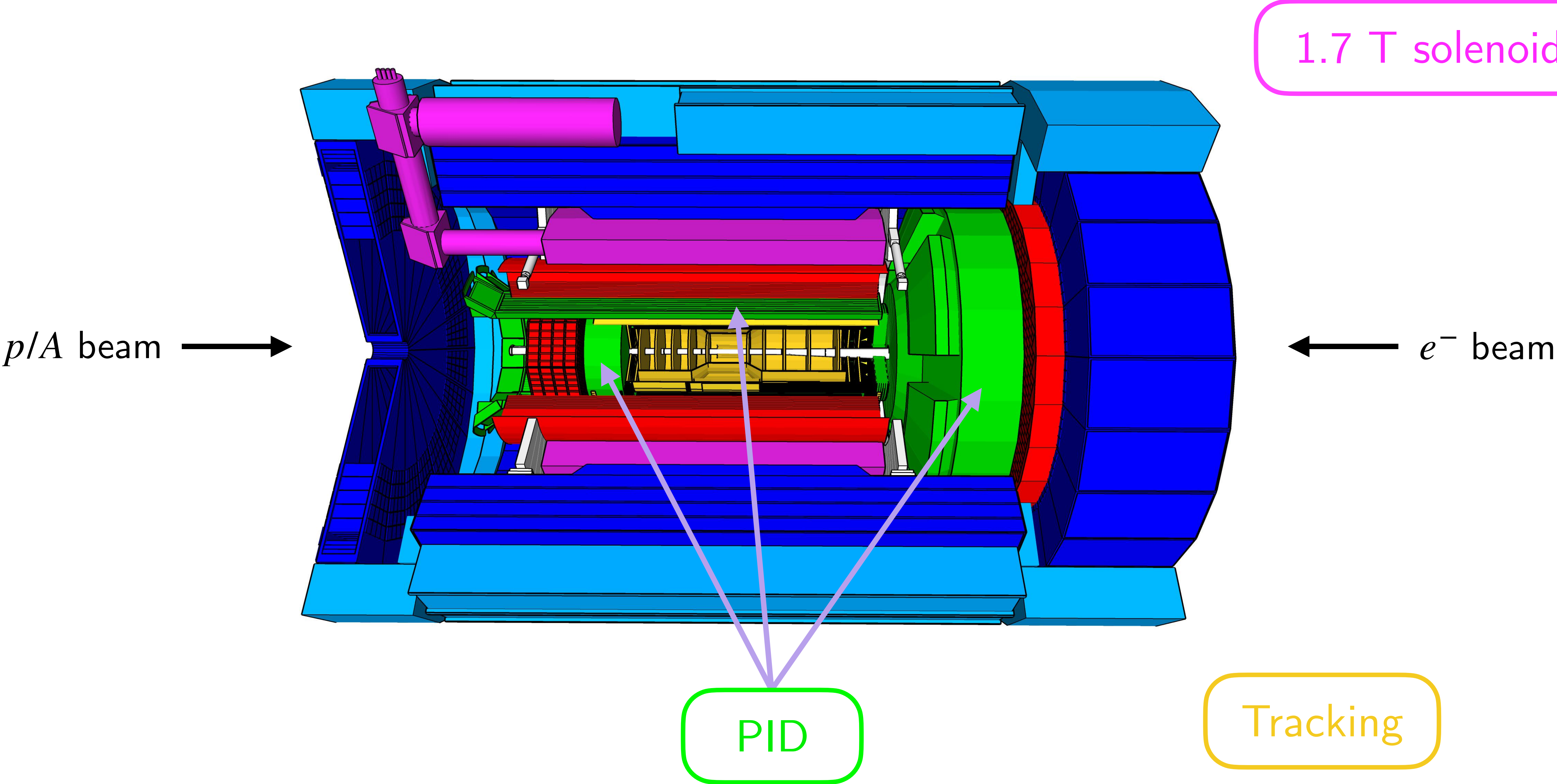
# ePIC designed to be hermetic, multi-purpose detector



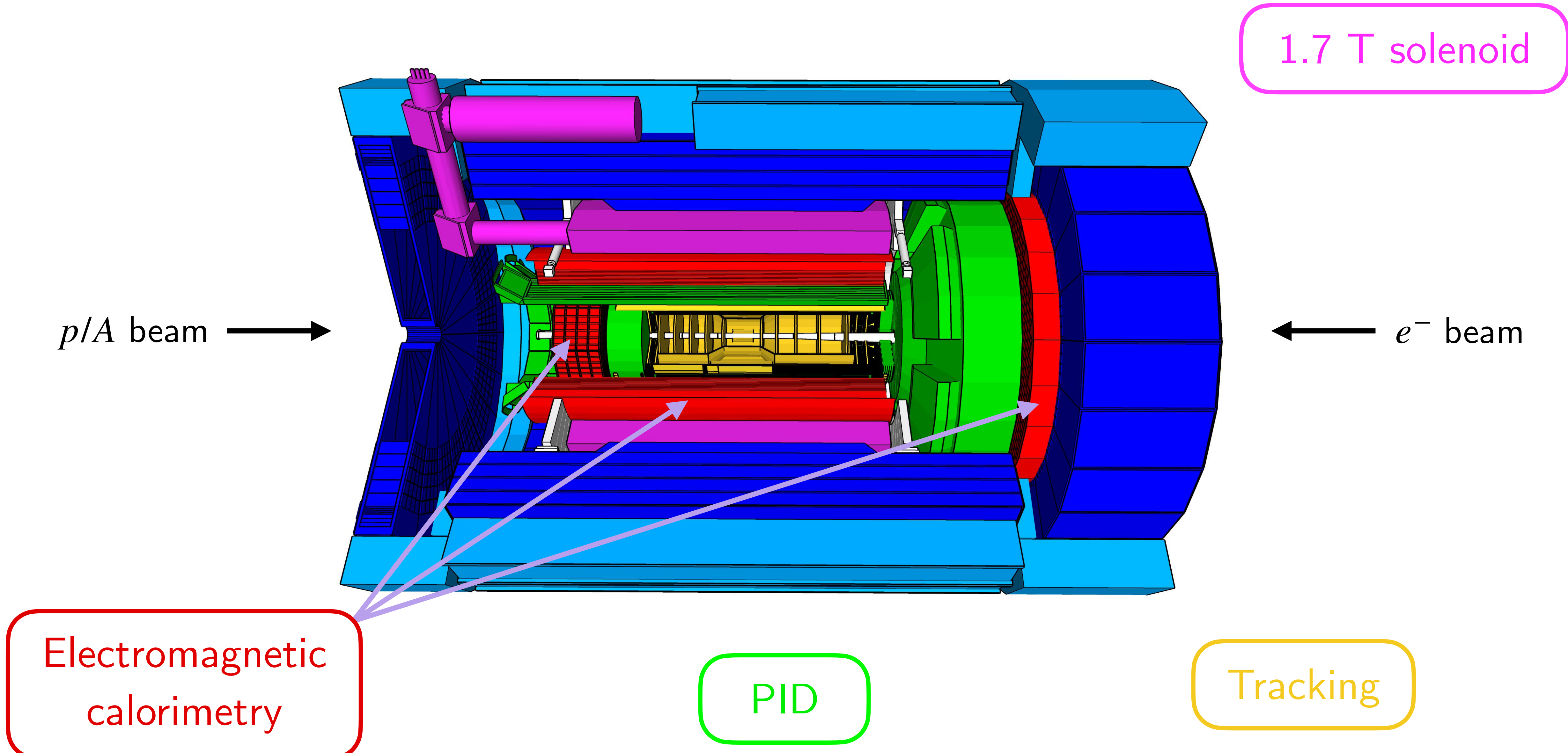
# ePIC designed to be hermetic, multi-purpose detector



# ePIC designed to be hermetic, multi-purpose detector



# ePIC designed to be hermetic, multi-purpose detector



1.7 T solenoid

$p/A$  beam →

←  $e^-$  beam

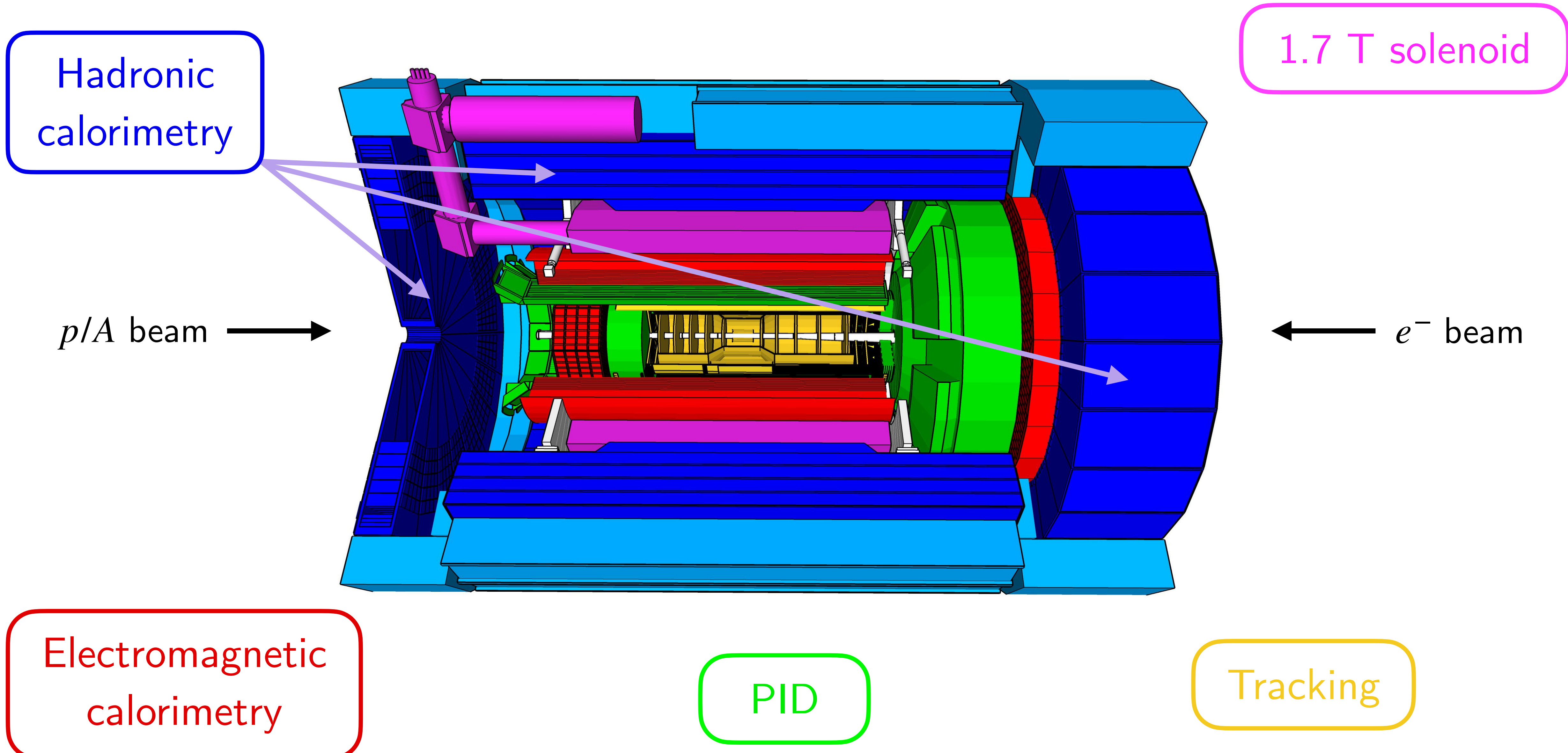
Electromagnetic calorimetry

PID

Tracking



# ePIC designed to be hermetic, multi-purpose detector



Hadronic calorimetry

1.7 T solenoid

$p/A$  beam →

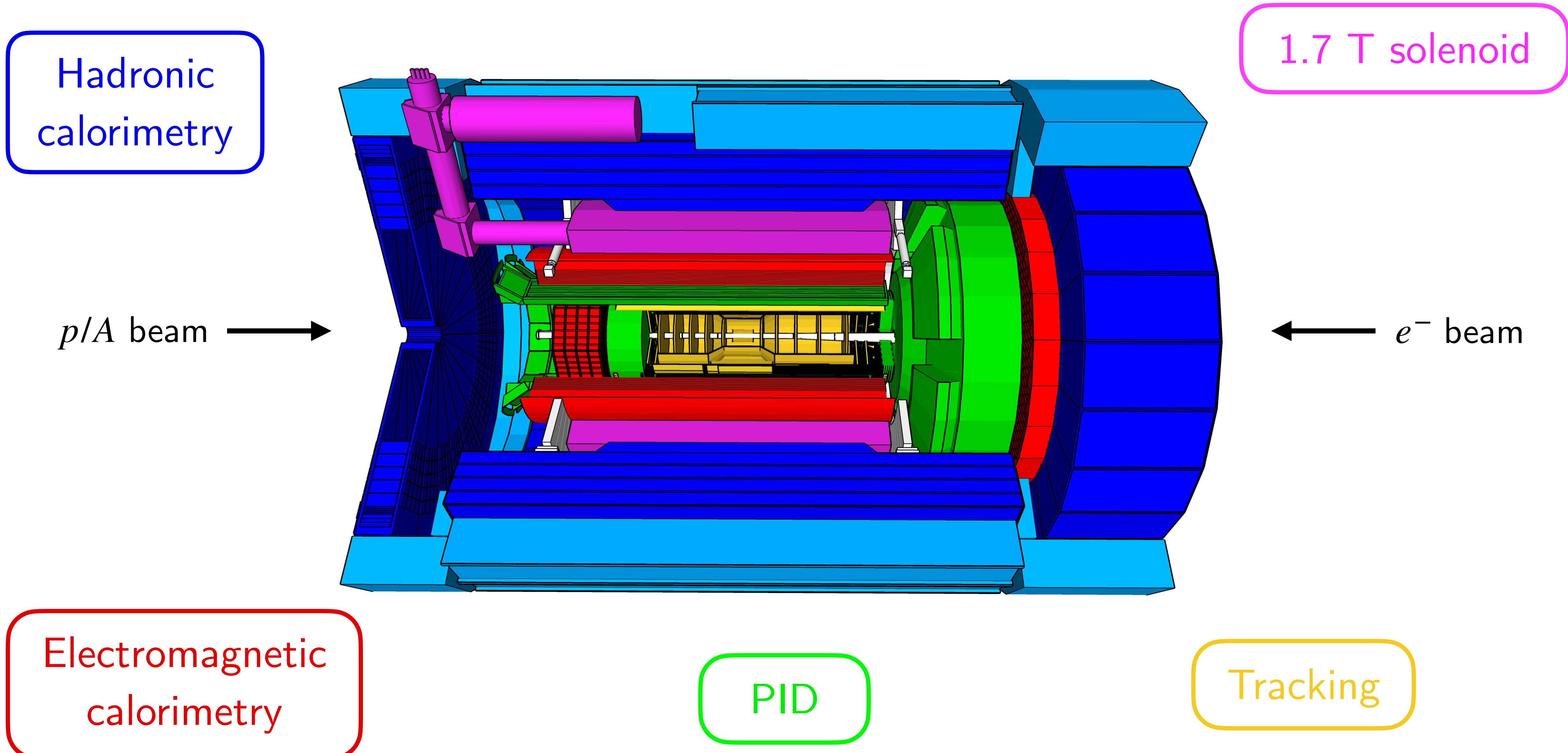
←  $e^-$  beam

Electromagnetic calorimetry

PID

Tracking

# ePIC designed to be hermetic, multi-purpose detector



# Motivation:

## some EIC observables and related systematics

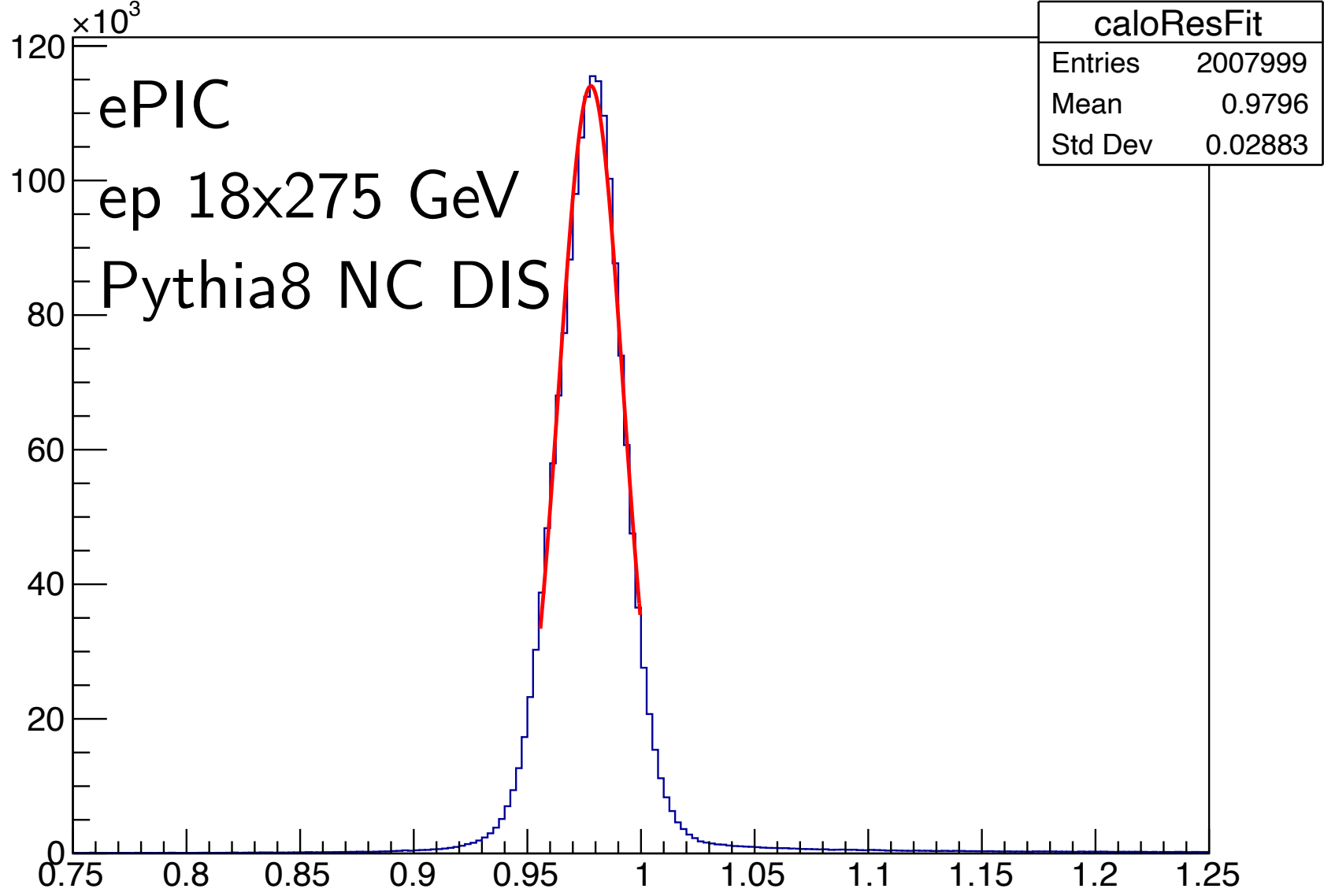
- Parity-violating asymmetries  $A_{PV}$
- $A_1^P$  from double-spin asymmetries
  - Limited by electron purity
  - $Q^2$  dependence critical!
- $F_L$  from reduced cross sections
- Fit  $y$  dependence for fixed  $(x_B, Q^2)$ 
  - Must combine multiple beam energies
  - $\pi$  contamination depends strongly on  $y$

# Overview

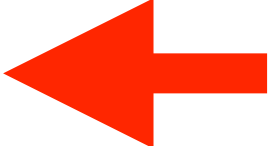
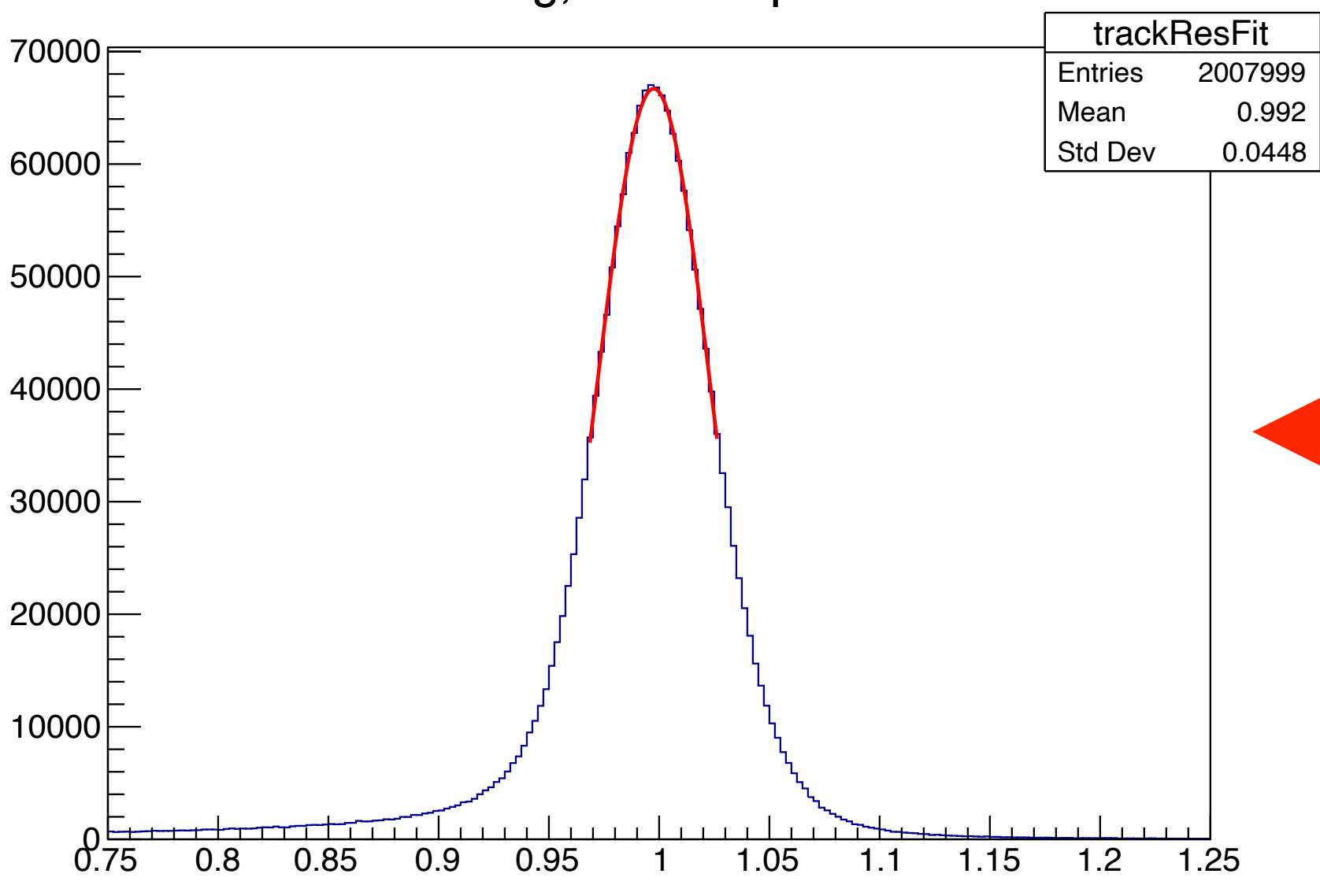
- Electron energy resolutions
- Calibration of electromagnetic calorimeters
- Kinematic reconstruction
- Electron identification and purity
- Luminosity & polarization

# Electron momentum resolutions

Calorimetry,  $-2.60 < \eta < -2.20$

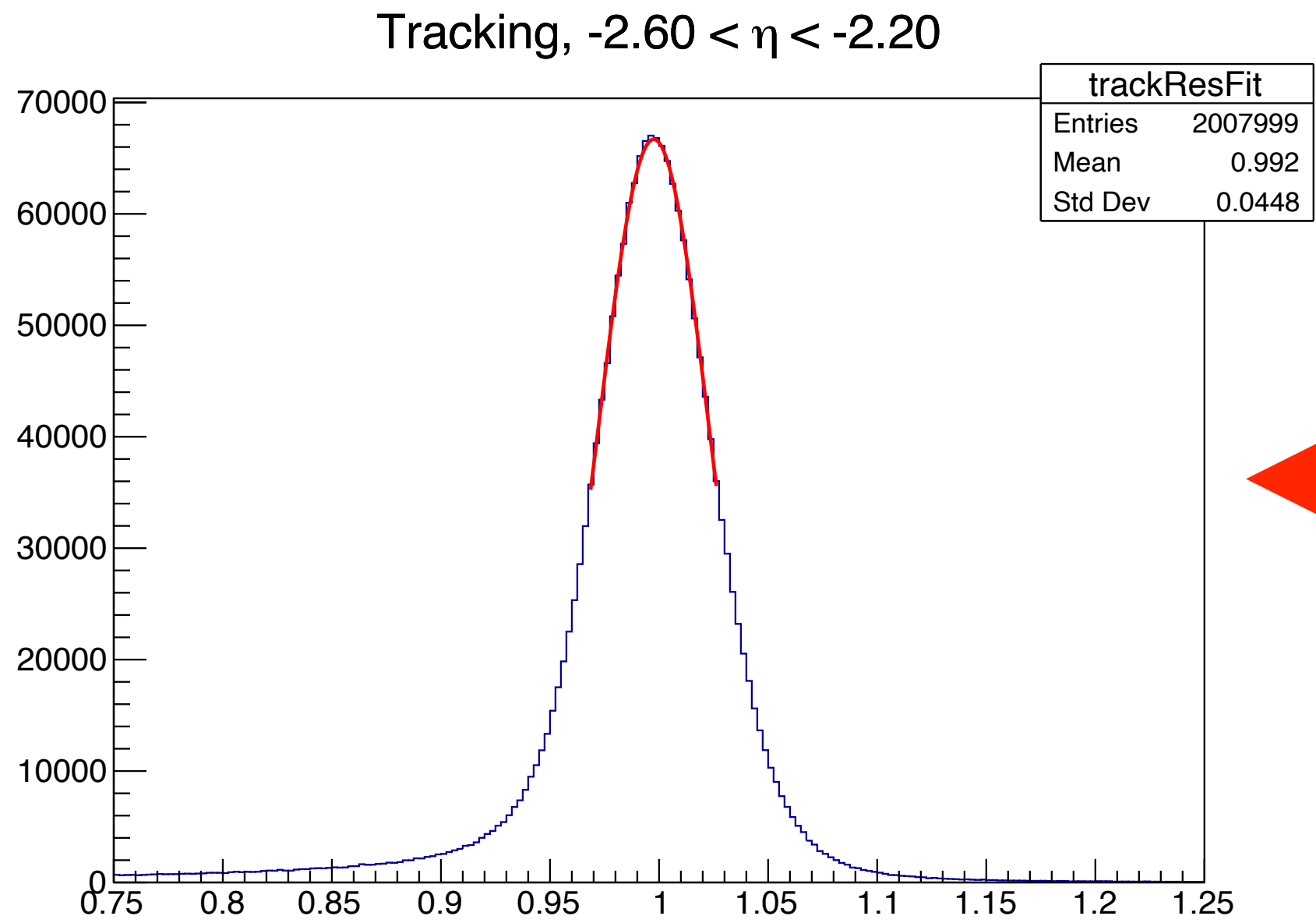
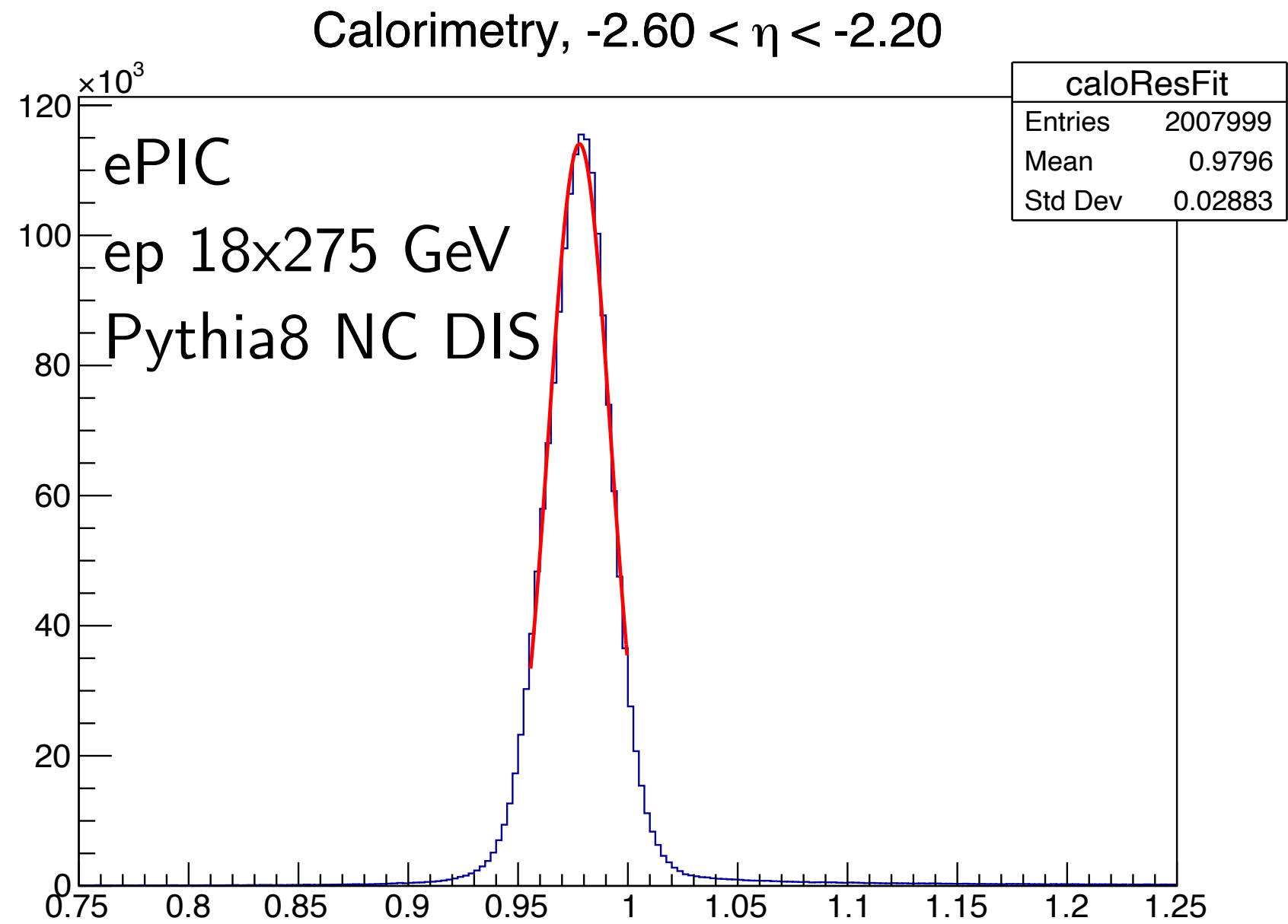


Tracking,  $-2.60 < \eta < -2.20$

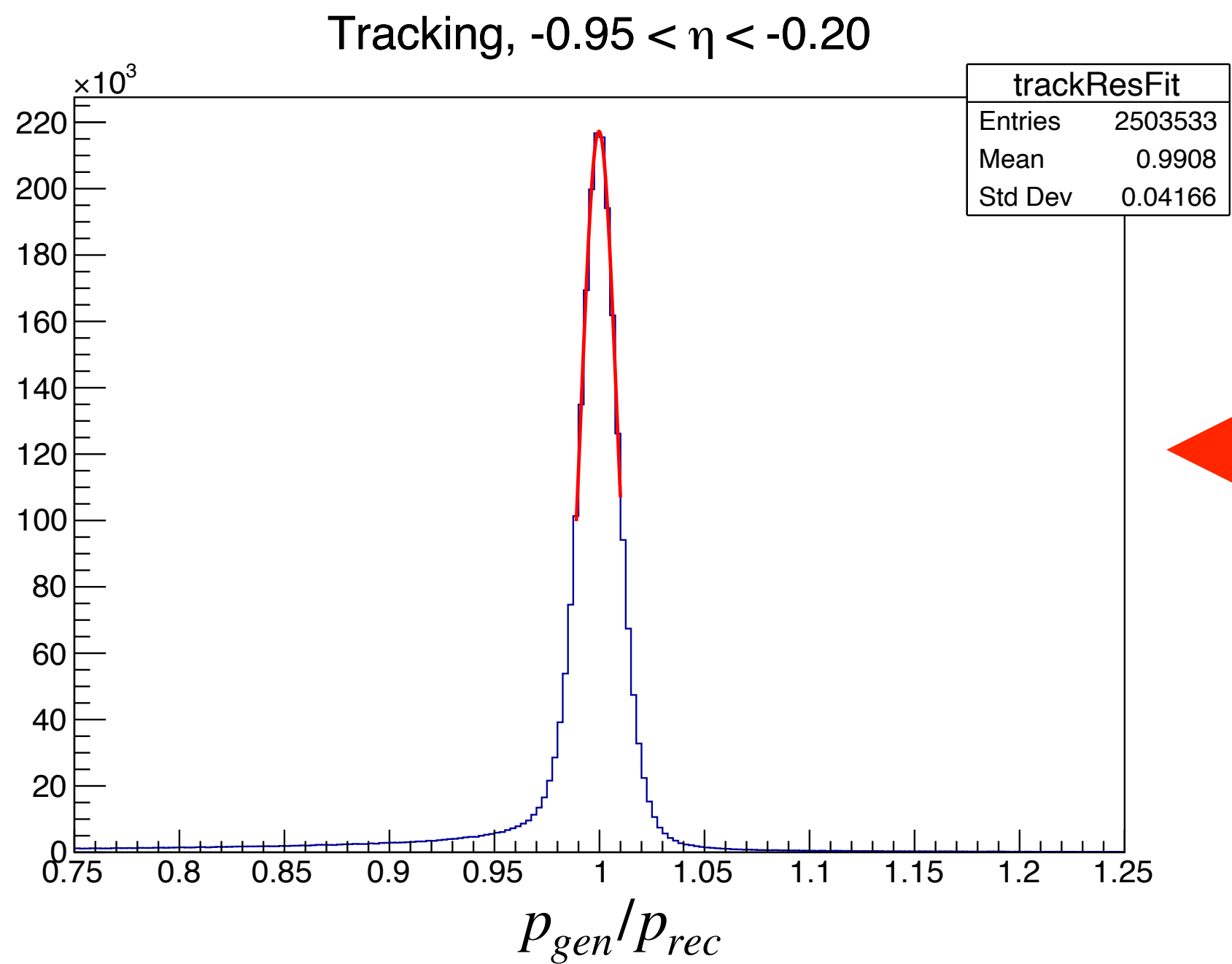
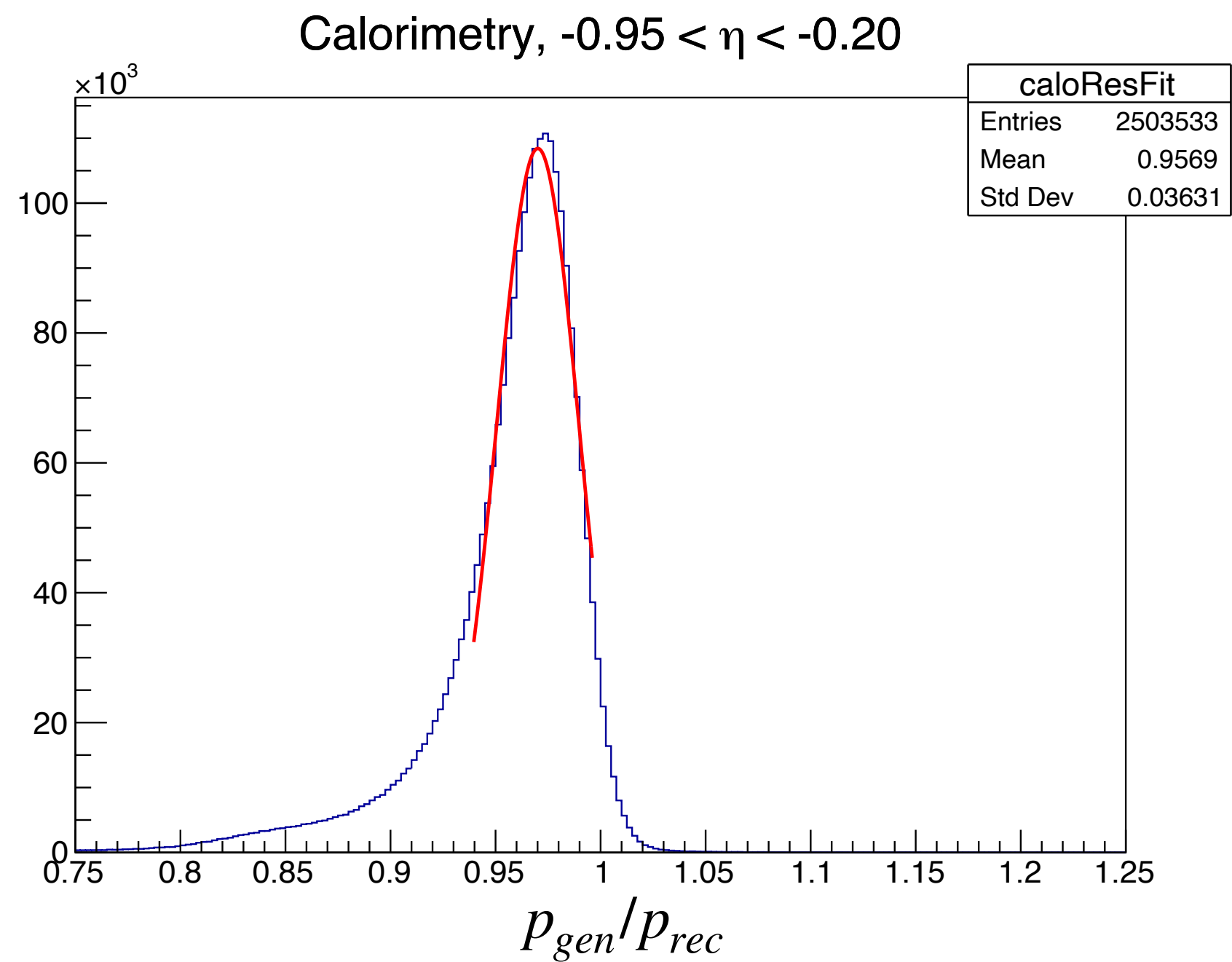


Calorimeter resolution  
better in endcap

# Electron momentum resolutions

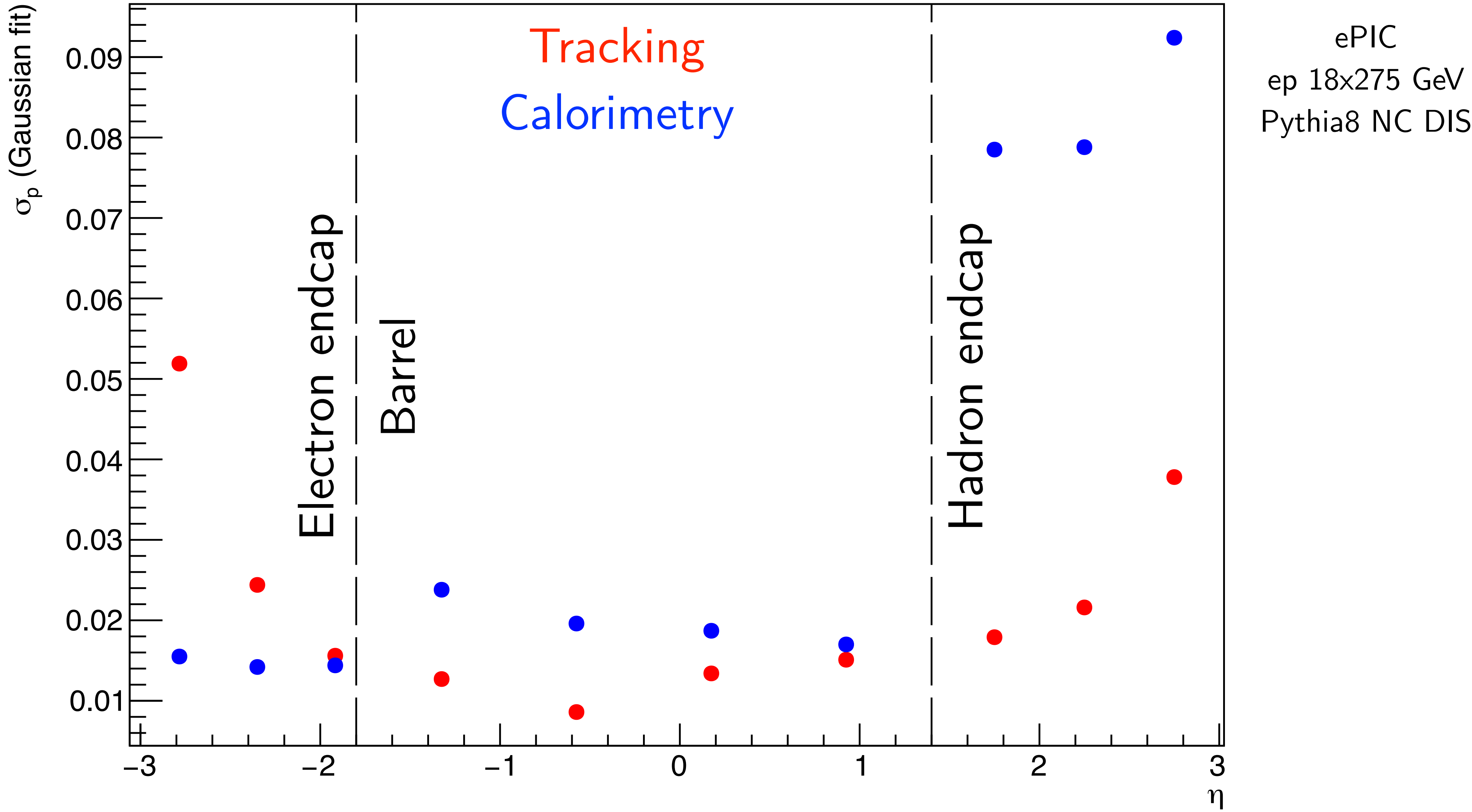


← Calorimeter resolution  
better in endcap

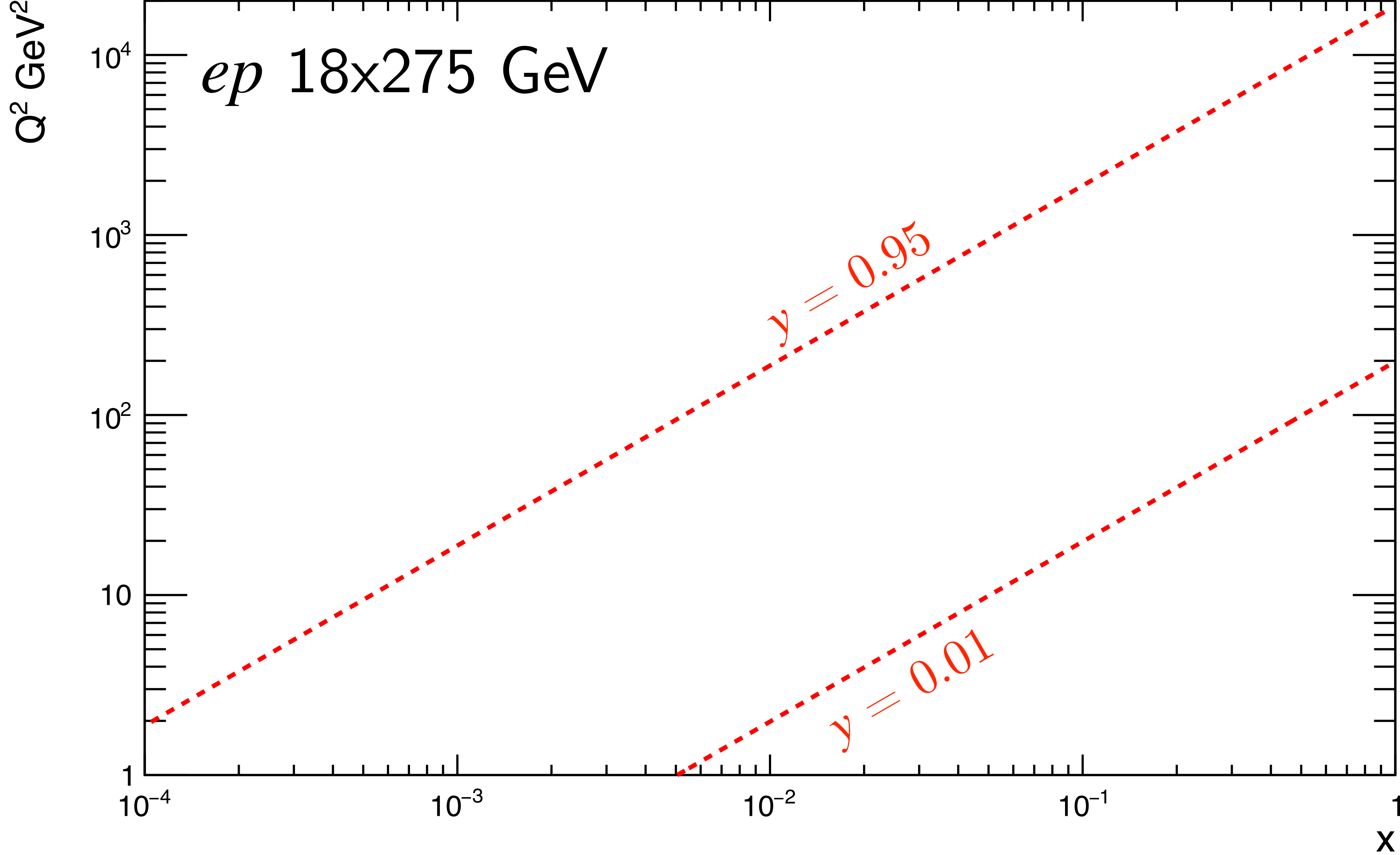


← Tracking resolution  
better in barrel

# Electron momentum resolutions across $\eta$

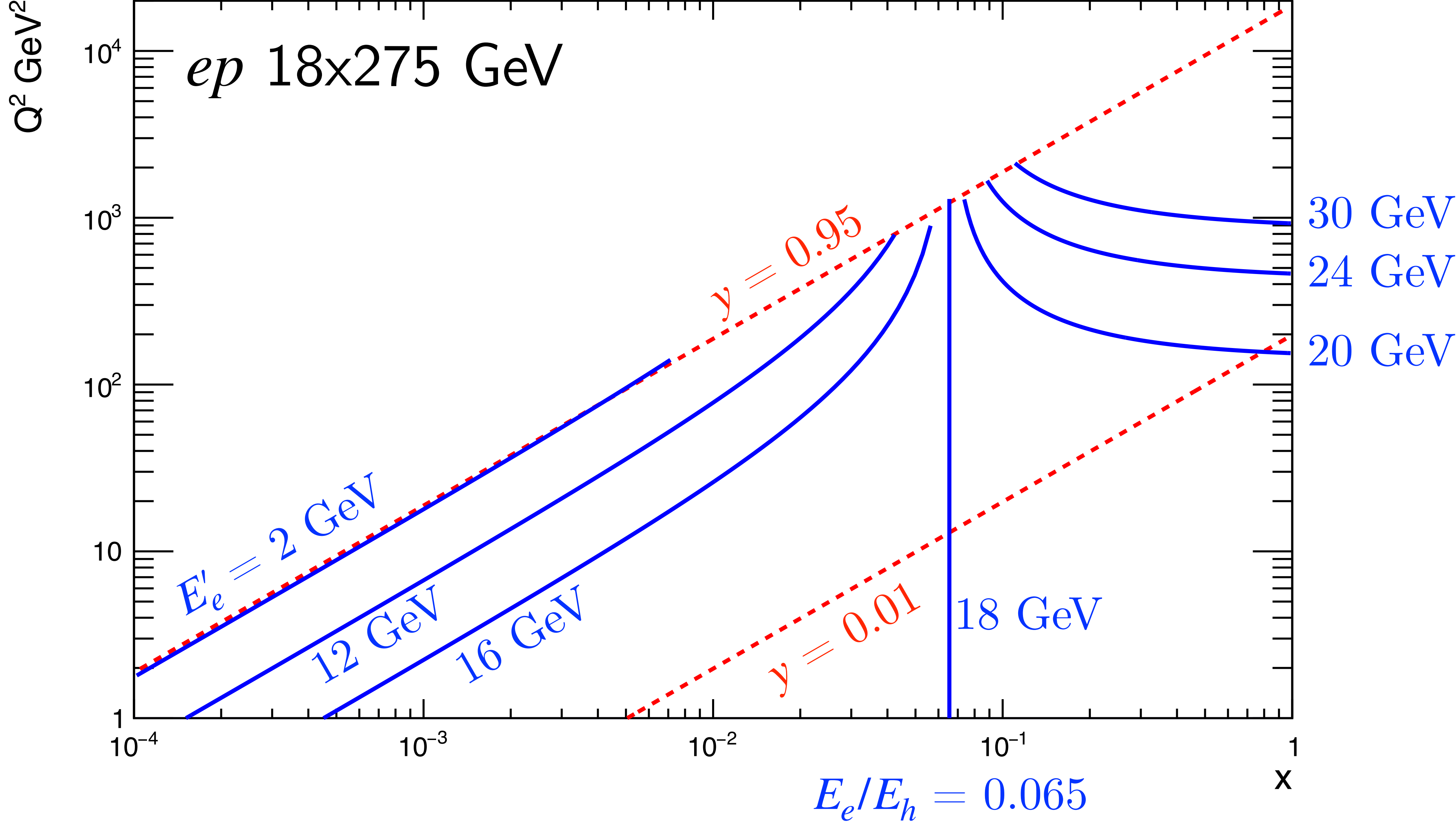


# Kinematic peak method for ECAL calibration

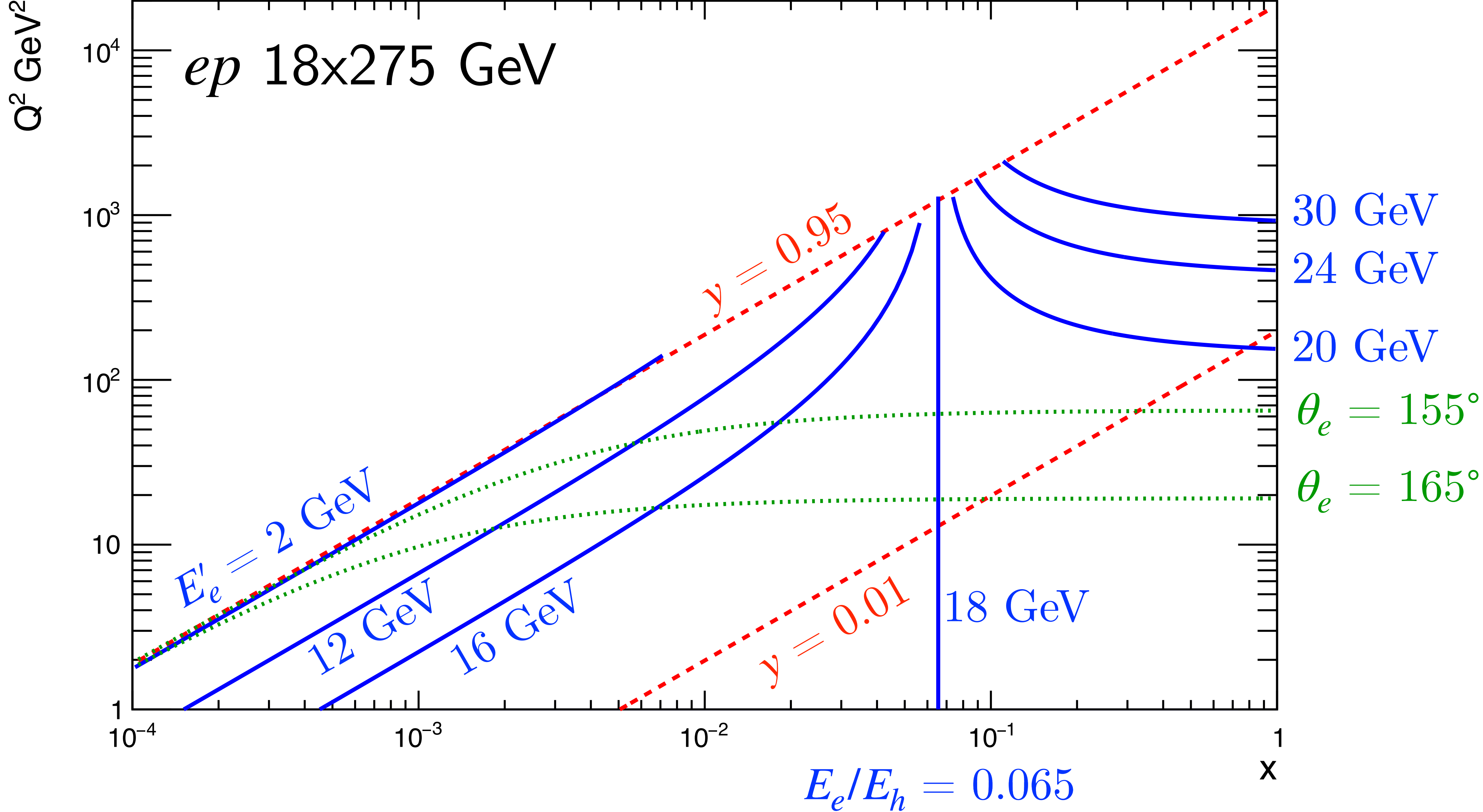




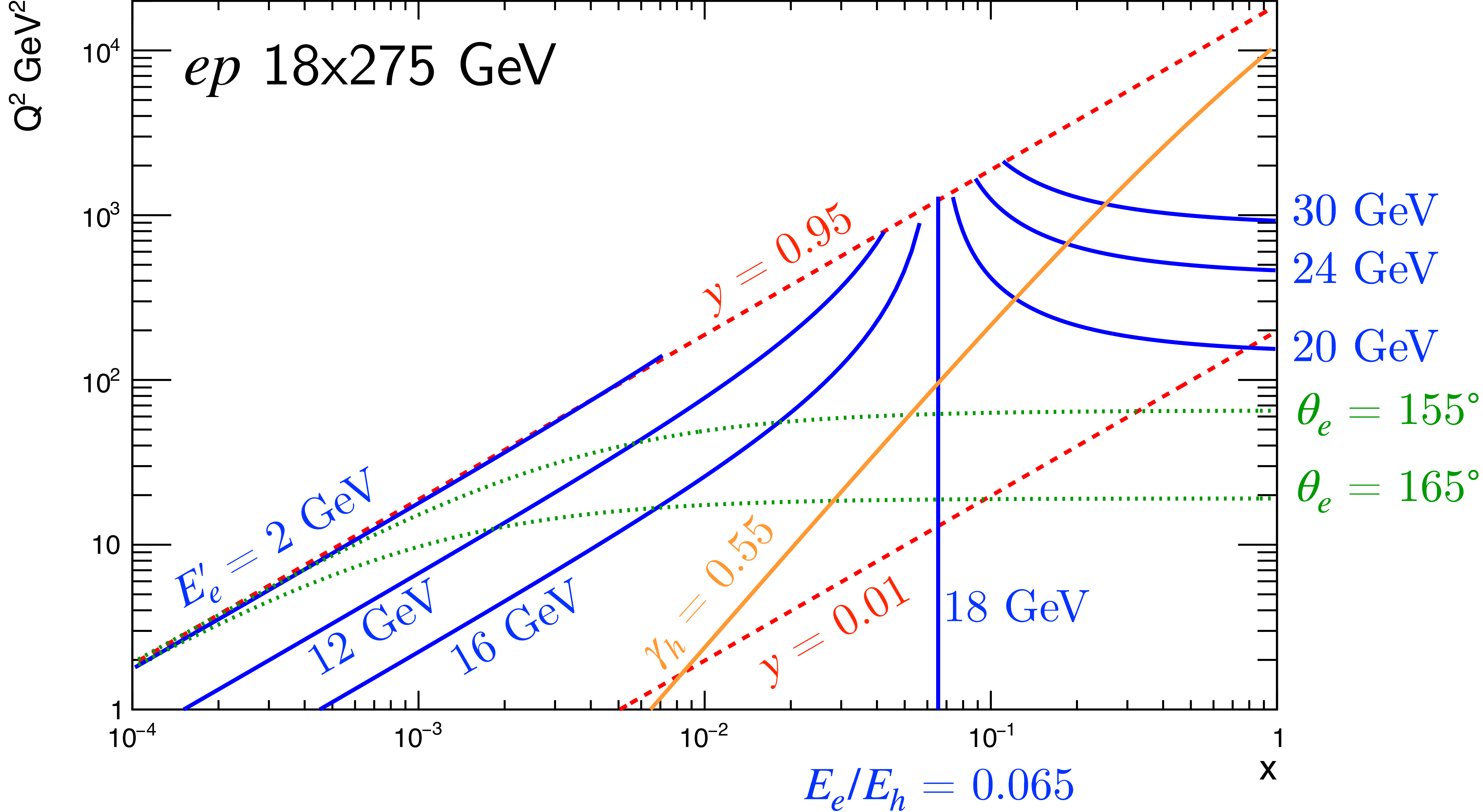
# Kinematic peak method for ECAL calibration



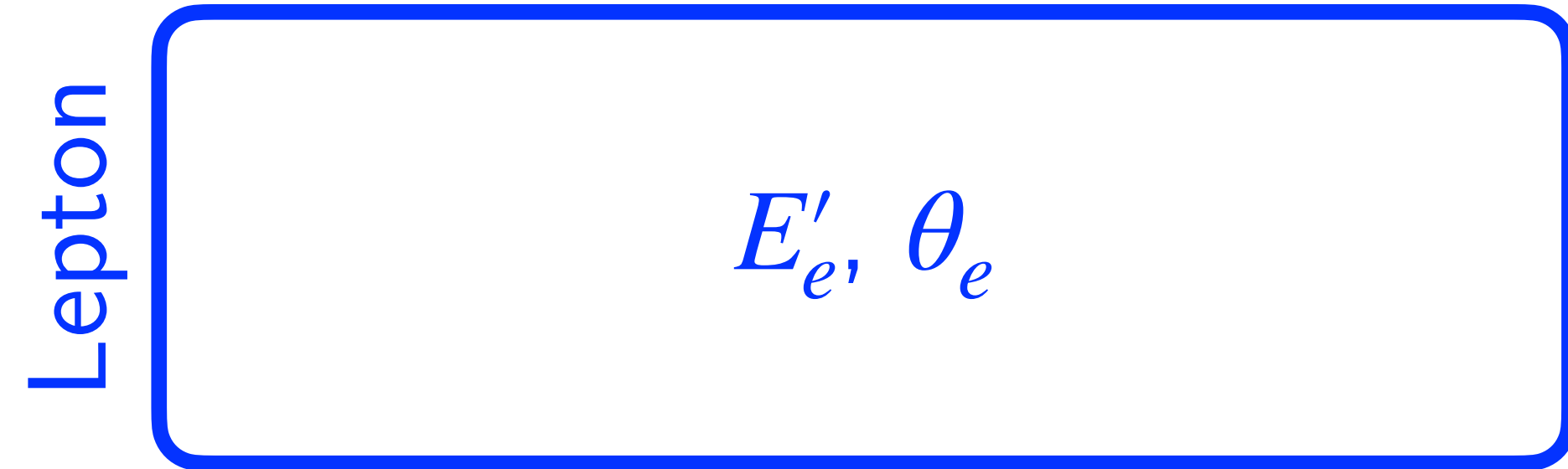
# Kinematic peak method for ECAL calibration



# Kinematic peak method for ECAL calibration



Traditional reconstruction methods use subset of lepton, hadron quantities



Traditional reconstruction methods use subset of lepton, hadron quantities

Lepton

$$E'_e, \theta_e$$

- Electron

$$Q^2 (E'_e, \theta_e), y (E'_e, \theta_e)$$

# Traditional reconstruction methods use subset of lepton, hadron quantities

Lepton

$$E'_e, \theta_e$$

Hadron

$$\delta_h = \sum_i (E_i - p_{z,i})$$

$$p_{T,h} = \sqrt{\left(\sum_i p_{x,i}\right)^2 + \left(\sum_i p_{y,i}\right)^2}$$

$$\cos \gamma_h = \frac{p_{T,h}^2 - \delta_h^2}{p_{T,h}^2 + \delta_h^2}$$

- Electron

$$Q^2 (E'_e, \theta_e), y (E'_e, \theta_e)$$

- Jacquet-Blondel

$$Q^2 (\delta_h, p_{T,h}), y (\delta_h, p_{T,h})$$

# Traditional reconstruction methods use subset of lepton, hadron quantities

Lepton

$$E'_e, \theta_e$$

Hadron

$$\delta_h = \sum_i (E_i - p_{z,i})$$

$$p_{T,h} = \sqrt{\left(\sum_i p_{x,i}\right)^2 + \left(\sum_i p_{y,i}\right)^2}$$

$$\cos \gamma_h = \frac{p_{T,h}^2 - \delta_h^2}{p_{T,h}^2 + \delta_h^2}$$

- Electron

$$Q^2 (E'_e, \theta_e), y (E'_e, \theta_e)$$

- Jacquet-Blondel

$$Q^2 (\delta_h, p_{T,h}), y (\delta_h, p_{T,h})$$

- Double-angle

$$Q^2 (\gamma_h, \theta_e), y (\gamma_h, \theta_e)$$

# Traditional reconstruction methods use subset of lepton, hadron quantities

Lepton

$$E'_e, \theta_e$$

Hadron

$$\delta_h = \sum_i (E_i - p_{z,i})$$

$$p_{T,h} = \sqrt{\left(\sum_i p_{x,i}\right)^2 + \left(\sum_i p_{y,i}\right)^2}$$

$$\cos \gamma_h = \frac{p_{T,h}^2 - \delta_h^2}{p_{T,h}^2 + \delta_h^2}$$

- Electron  
 $Q^2 (E'_e, \theta_e), y (E'_e, \theta_e)$
- Jacquet-Blondel  
 $Q^2 (\delta_h, p_{T,h}), y (\delta_h, p_{T,h})$
- Double-angle  
 $Q^2 (\gamma_h, \theta_e), y (\gamma_h, \theta_e)$
- $e\Sigma$   
 $Q^2 (E'_e, \theta_e), y (E'_e, \theta_e, \delta_h)$



Traditional reconstruction methods use subset of lepton, hadron quantities

Lepton

$$E'_e, \theta_e$$

Hadron

$$\delta_h = \sum_i (E_i - p_{z,i})$$

$$p_{T,h} = \sqrt{\left(\sum_i p_{x,i}\right)^2 + \left(\sum_i p_{y,i}\right)^2}$$

$$\cos \gamma_h = \frac{p_{T,h}^2 - \delta_h^2}{p_{T,h}^2 + \delta_h^2}$$

# Traditional reconstruction methods use subset of lepton, hadron quantities

Lepton

$$E'_e, \theta_e$$

Hadron

$$\delta_h = \sum_i (E_i - p_{z,i})$$

$$p_{T,h} = \sqrt{\left(\sum_i p_{x,i}\right)^2 + \left(\sum_i p_{y,i}\right)^2}$$

$$\cos \gamma_h = \frac{p_{T,h}^2 - \delta_h^2}{p_{T,h}^2 + \delta_h^2}$$

- Neutral-current analyses can leverage over-constrained kinematics to optimize resolution

# Traditional reconstruction methods use subset of lepton, hadron quantities

Lepton

$$E'_e, \theta_e$$

Hadron

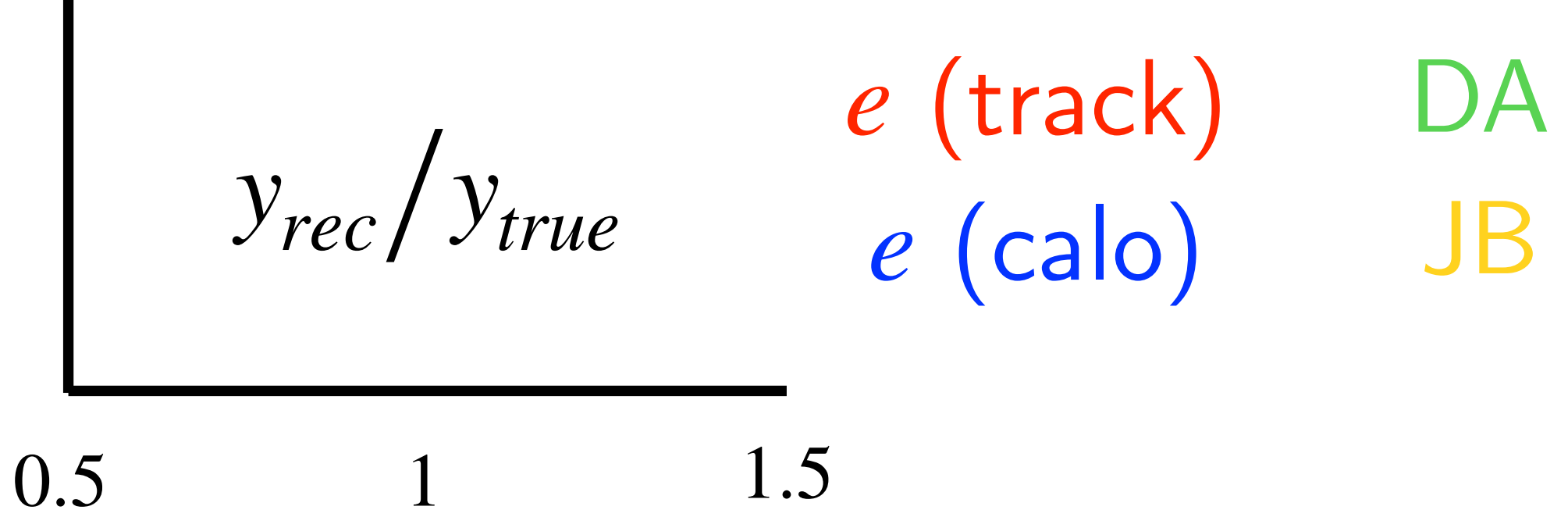
$$\delta_h = \sum_i (E_i - p_{z,i})$$

$$p_{T,h} = \sqrt{\left(\sum_i p_{x,i}\right)^2 + \left(\sum_i p_{y,i}\right)^2}$$

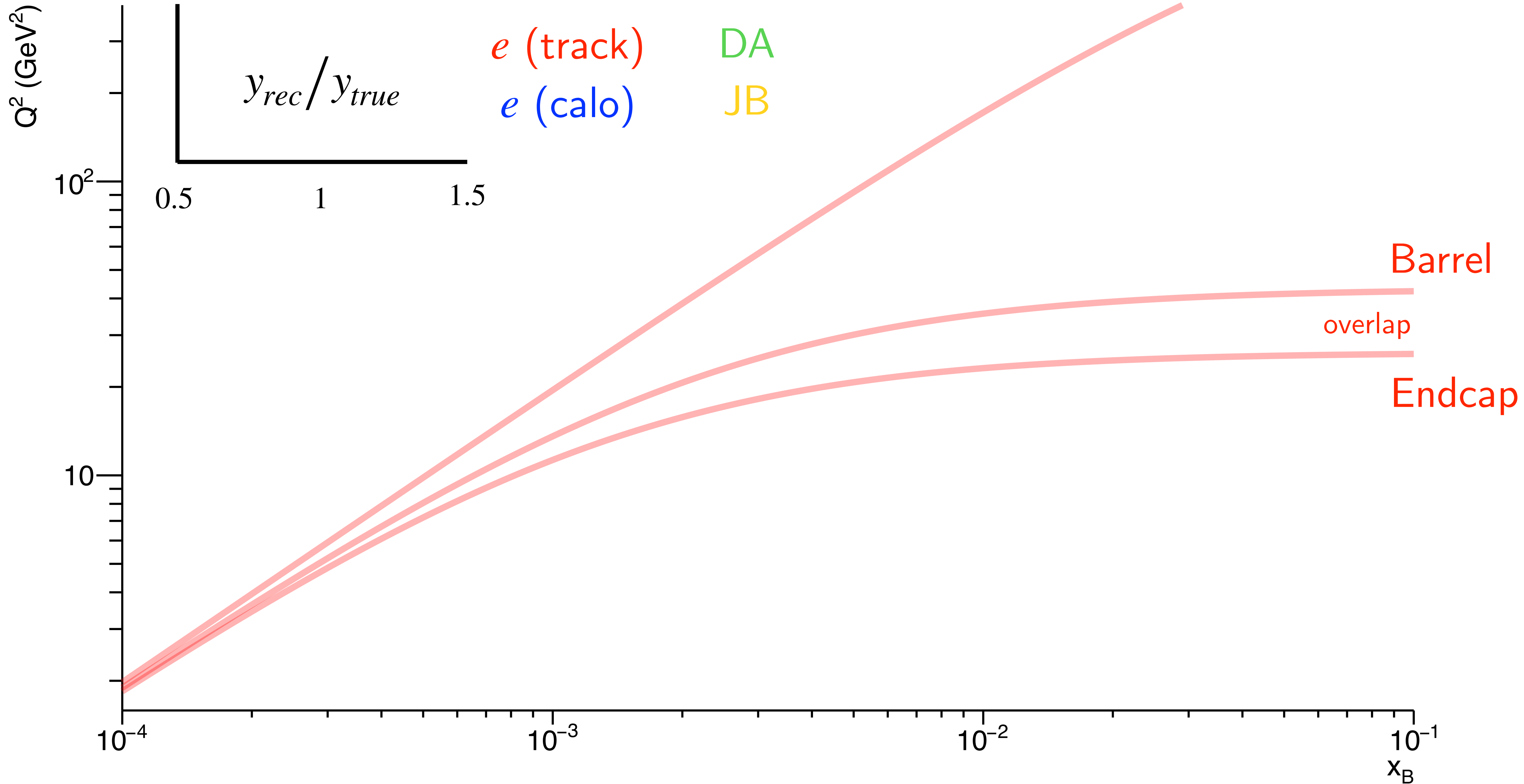
$$\cos \gamma_h = \frac{p_{T,h}^2 - \delta_h^2}{p_{T,h}^2 + \delta_h^2}$$

- Neutral-current analyses can leverage over-constrained kinematics to optimize resolution
- Hadronic final state:
  - *Only* option for charged-current analyses
  - PID needed to determine mass
  - Electron ID needed to eliminate scattered electron (and veto NC)

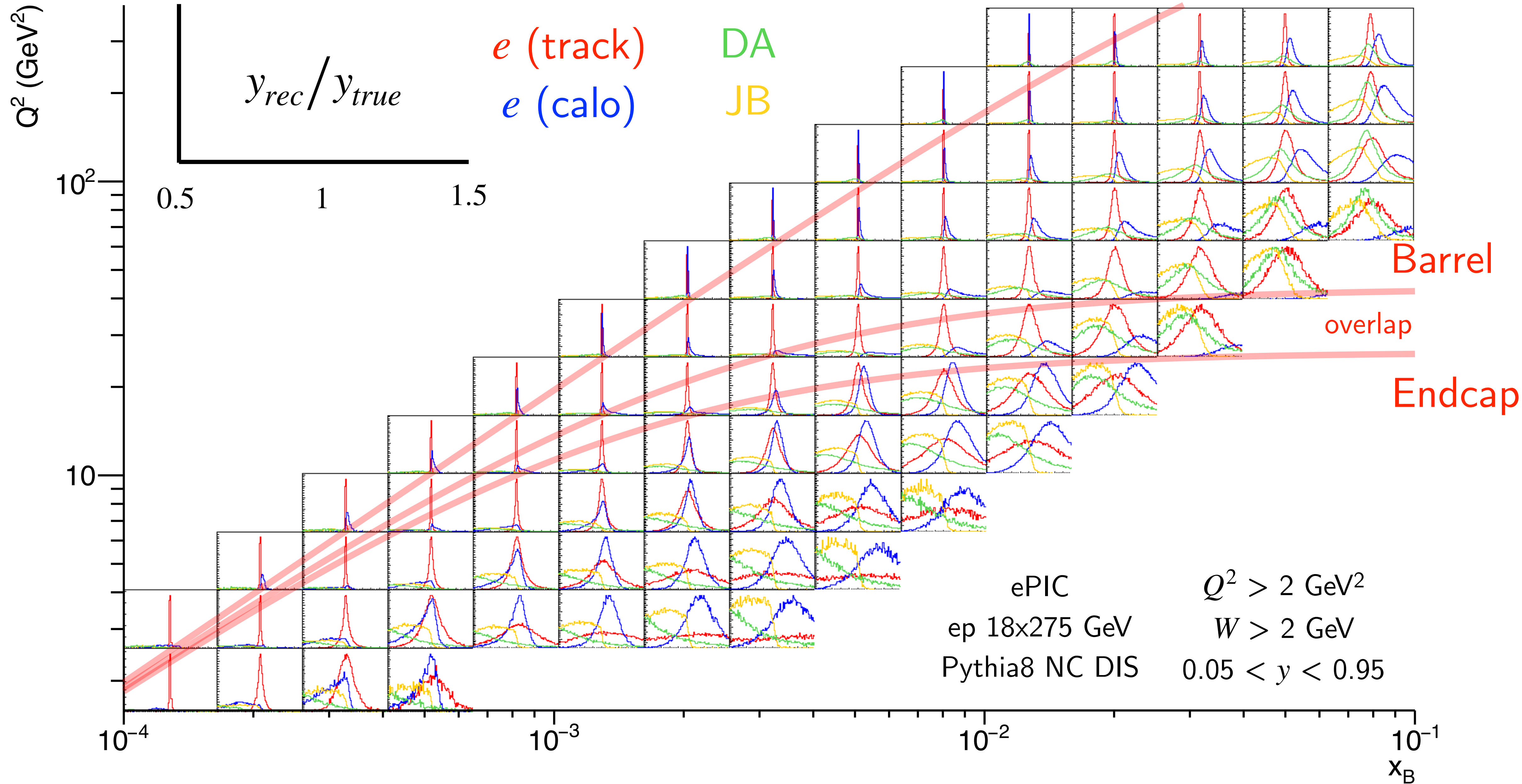
# Kinematic resolutions



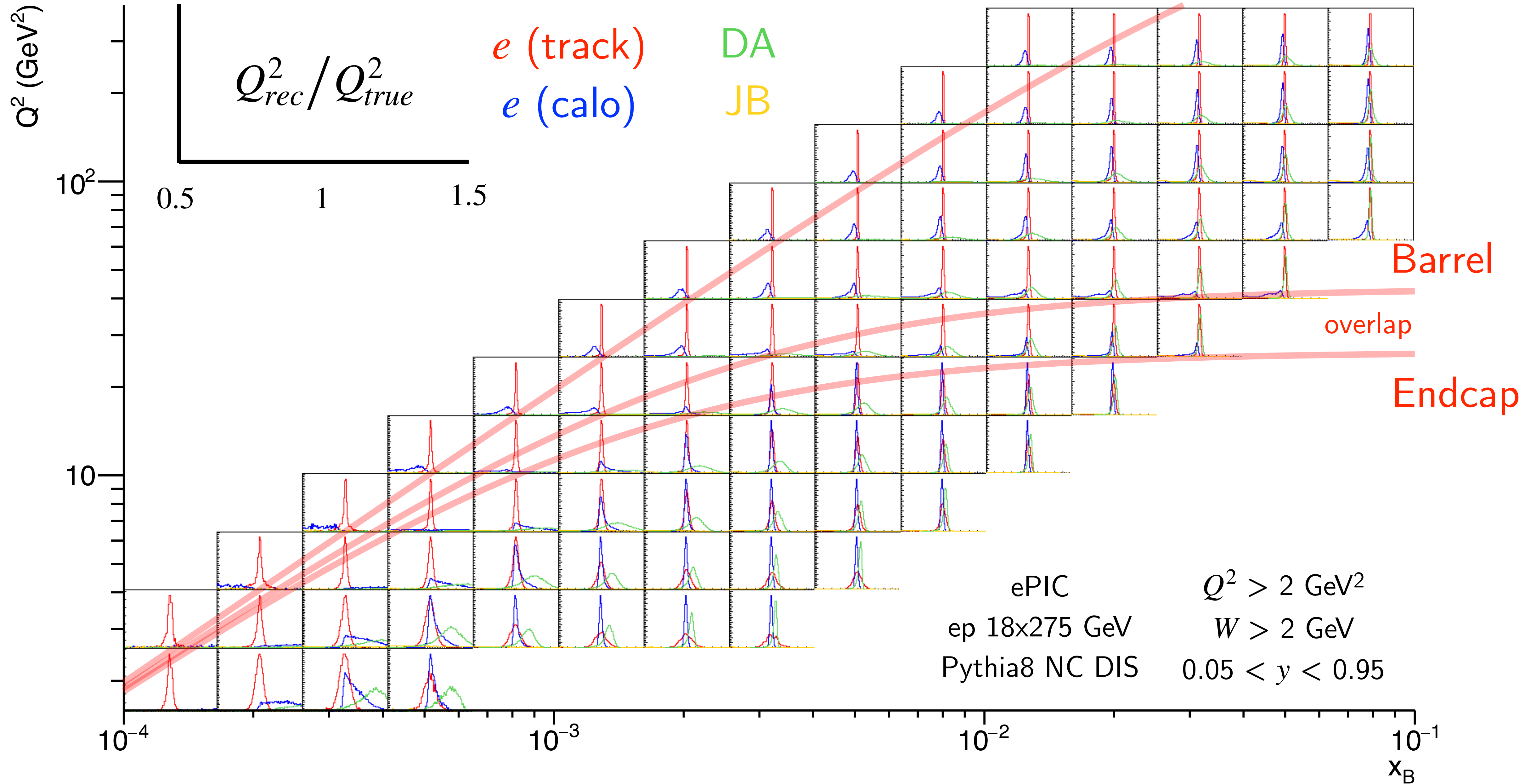
# Kinematic resolutions



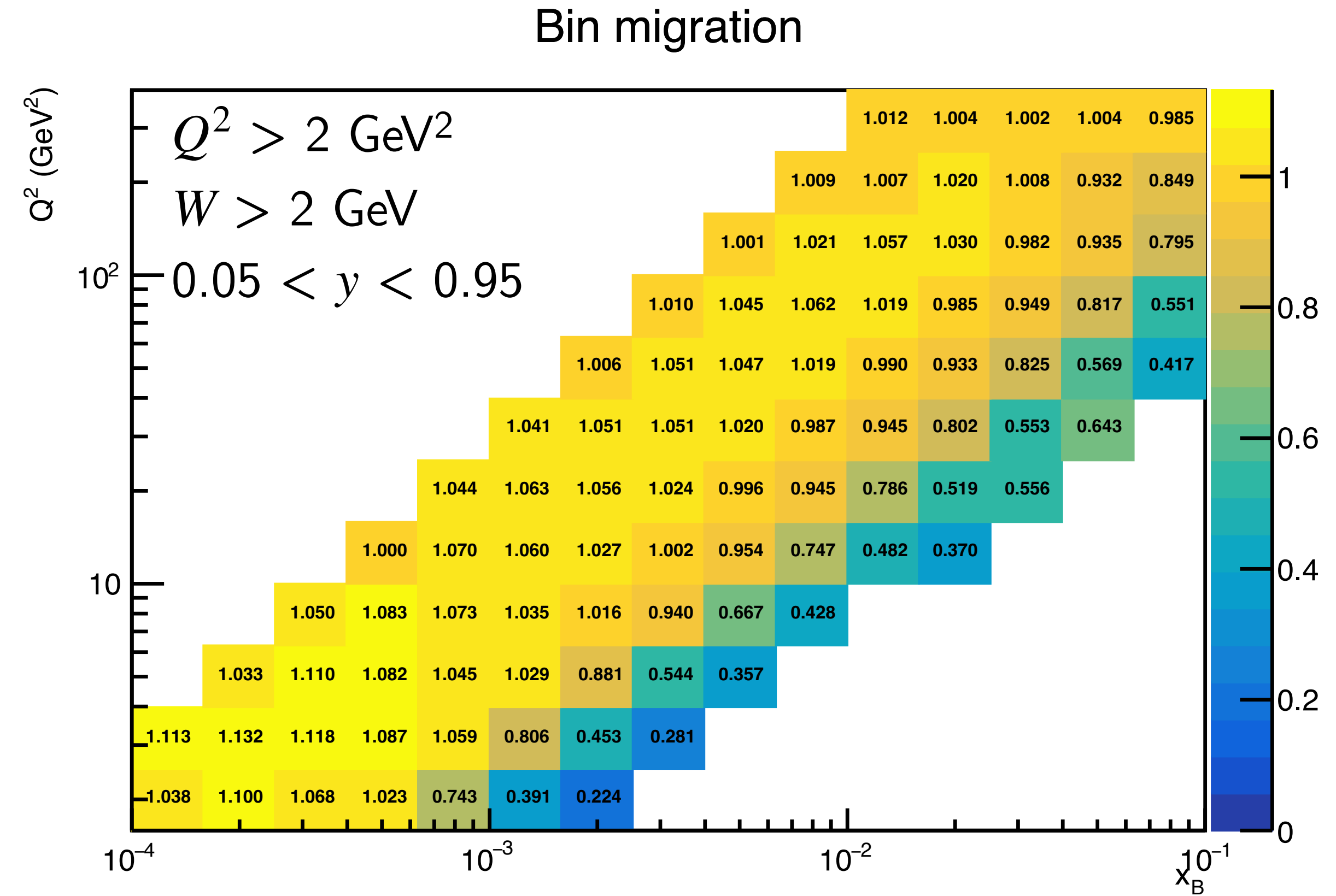
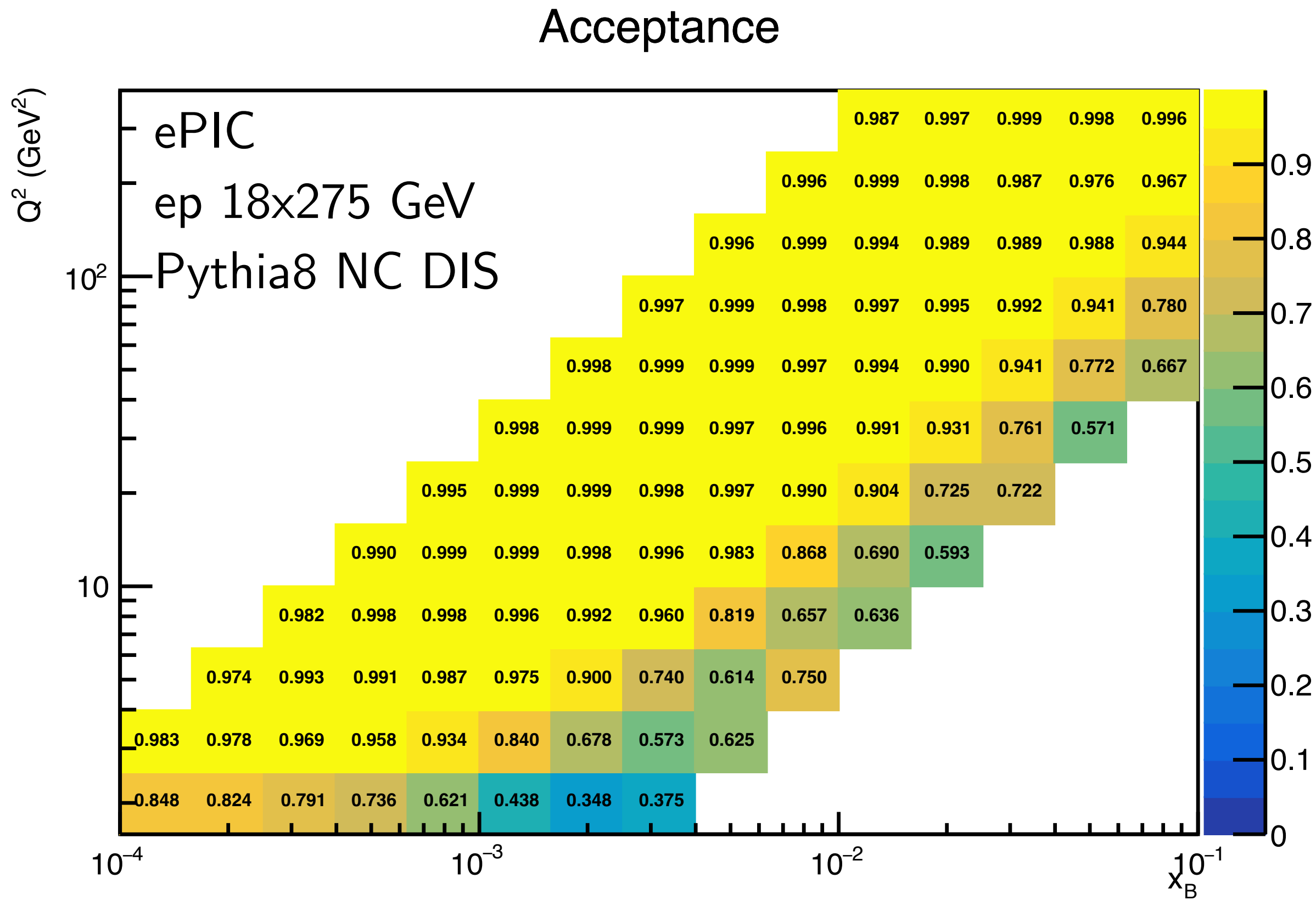
# Kinematic resolutions



# Kinematic resolutions



# Acceptance and bin migration (electron track)

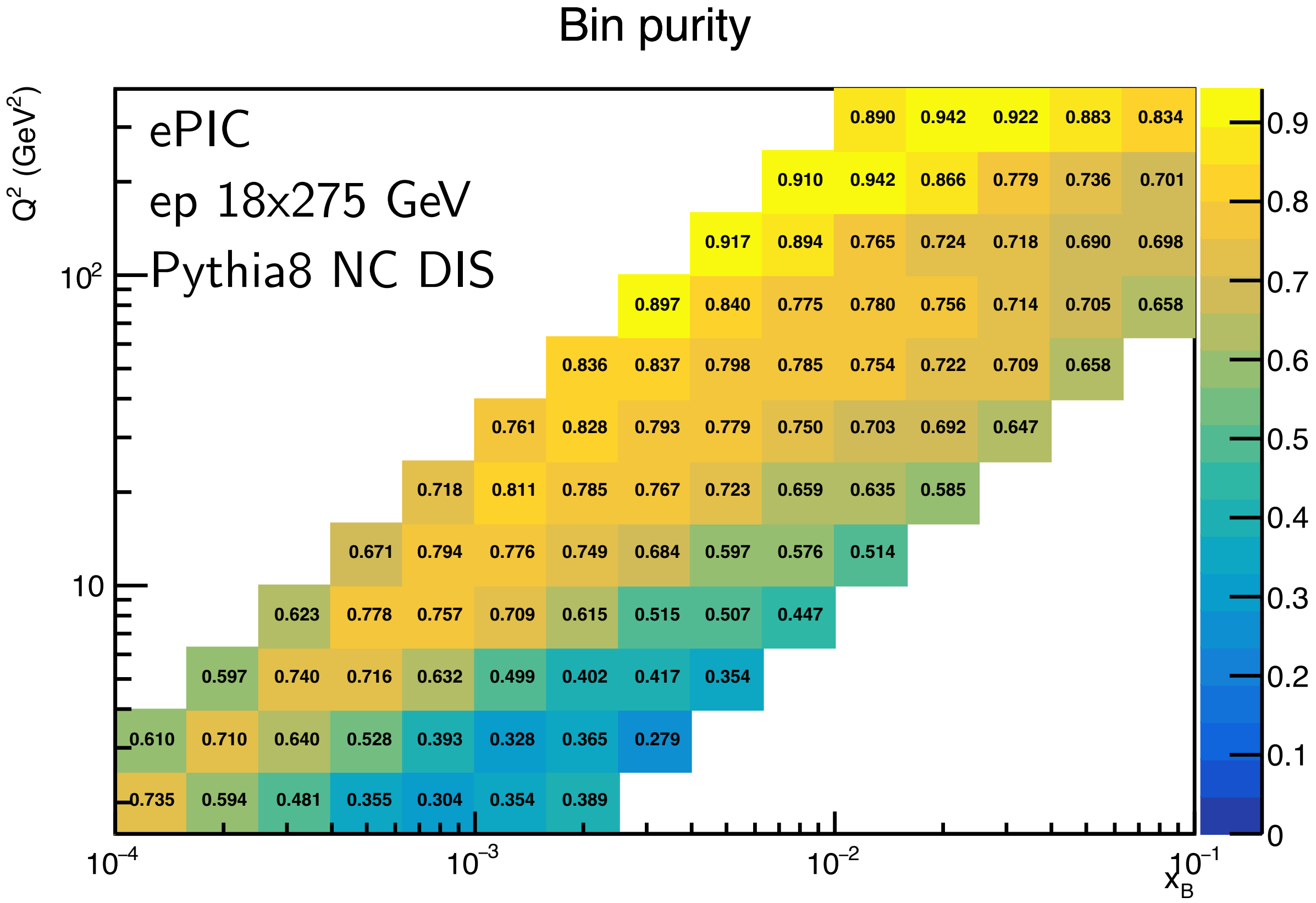


$$C_{acc} = \frac{N_{rec}(x_{gen}, Q_{gen}^2)}{N_{gen}(x_{gen}, Q_{gen}^2)}$$

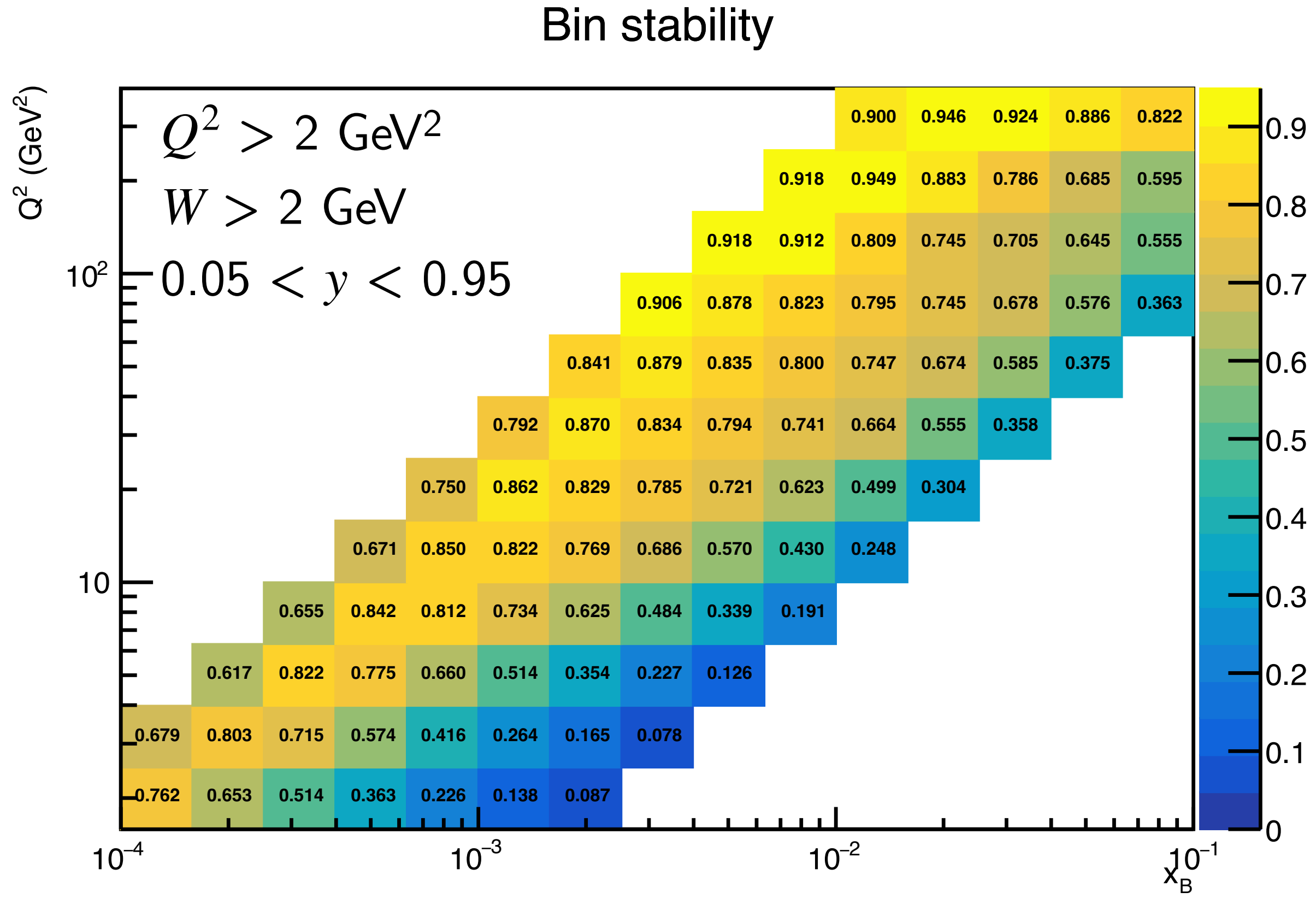
$$C_{bin} = \frac{N_{rec}(x_{rec}, Q_{rec}^2)}{N_{rec}(x_{gen}, Q_{gen}^2)}$$



# Bin stability and purity (electron track)

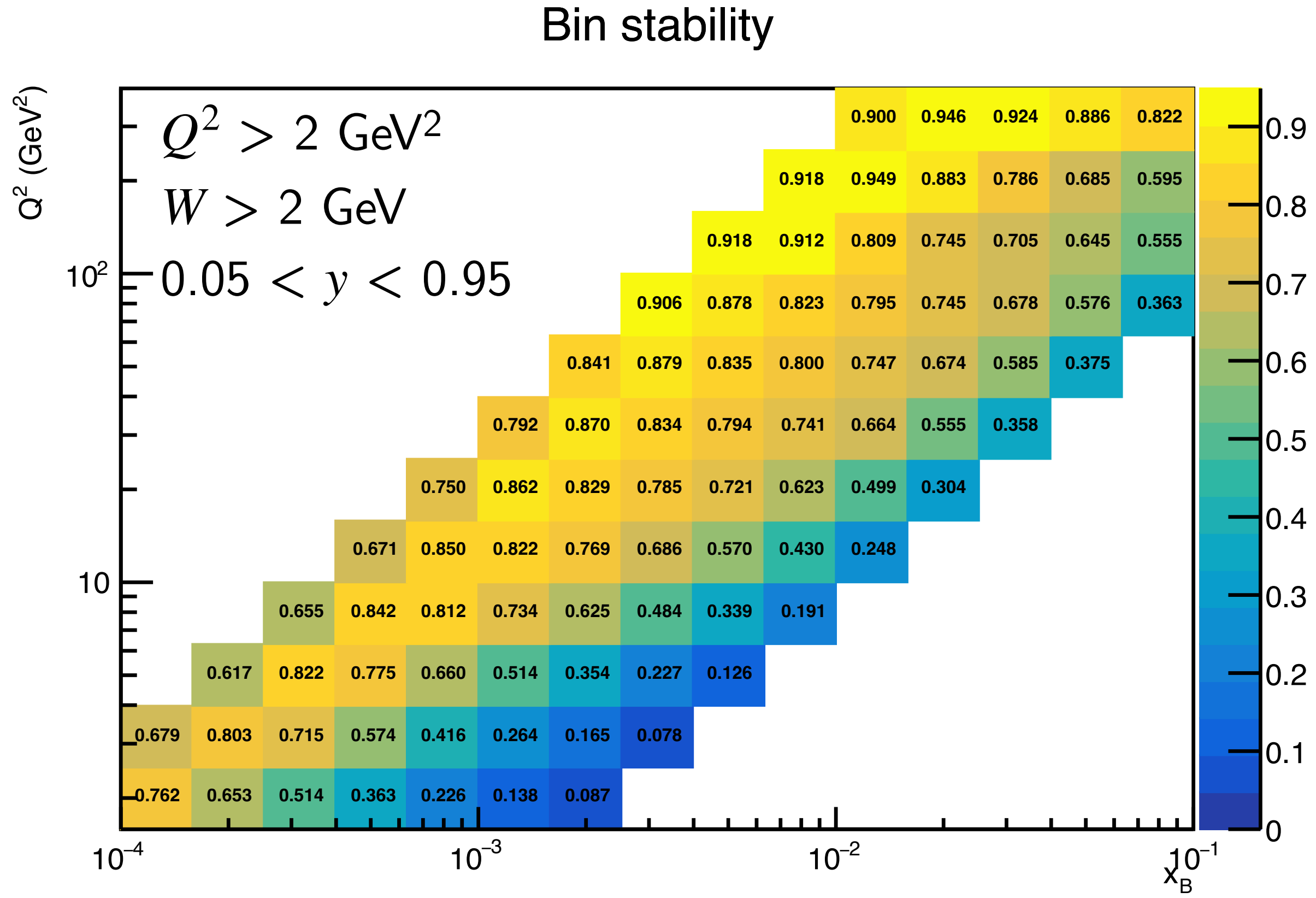
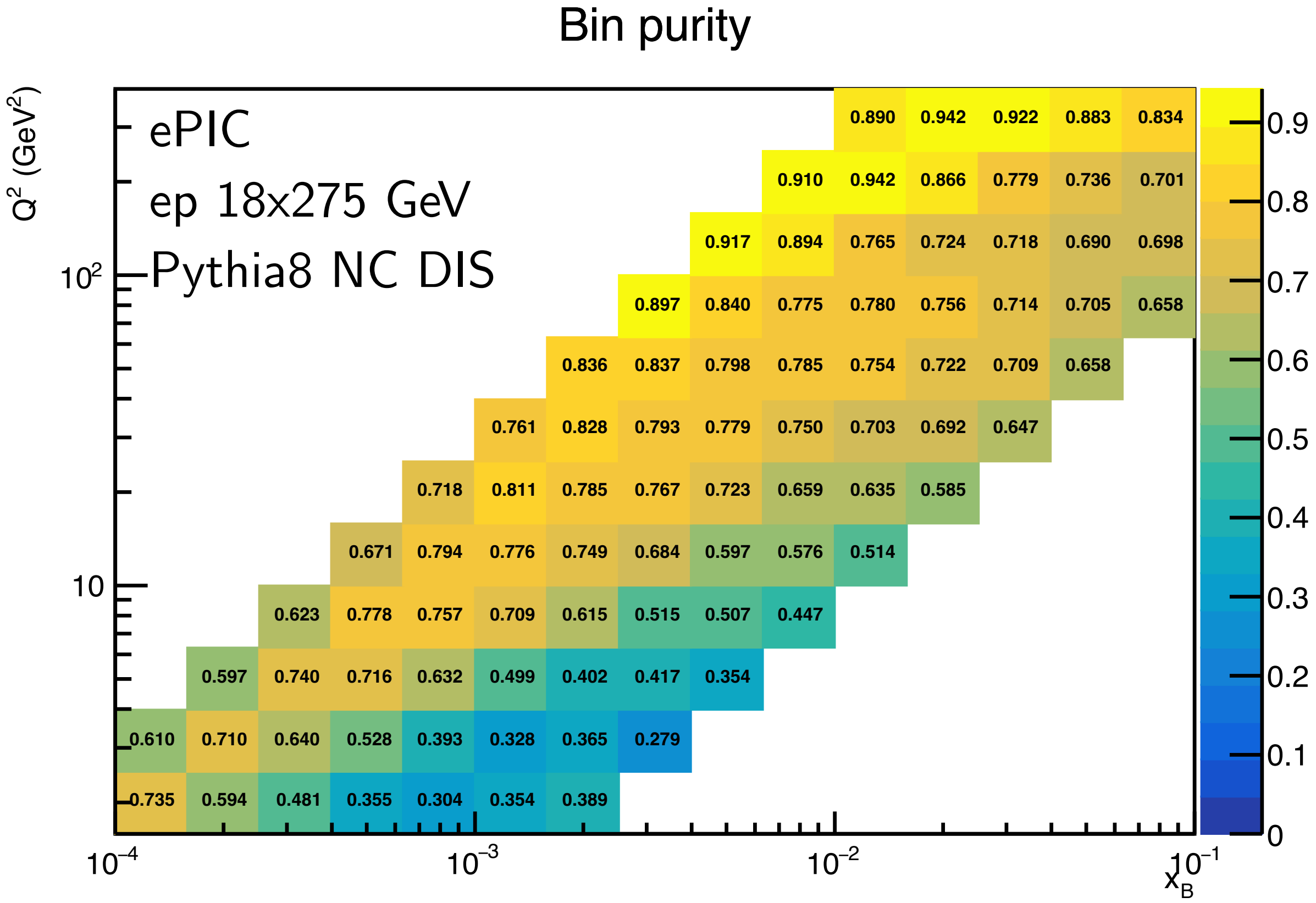


$$P = \frac{N_{gen+rec}}{N_{rec}}$$



$$S = \frac{N_{gen+rec}}{N_{gen}}$$

# Bin stability and purity (electron track)

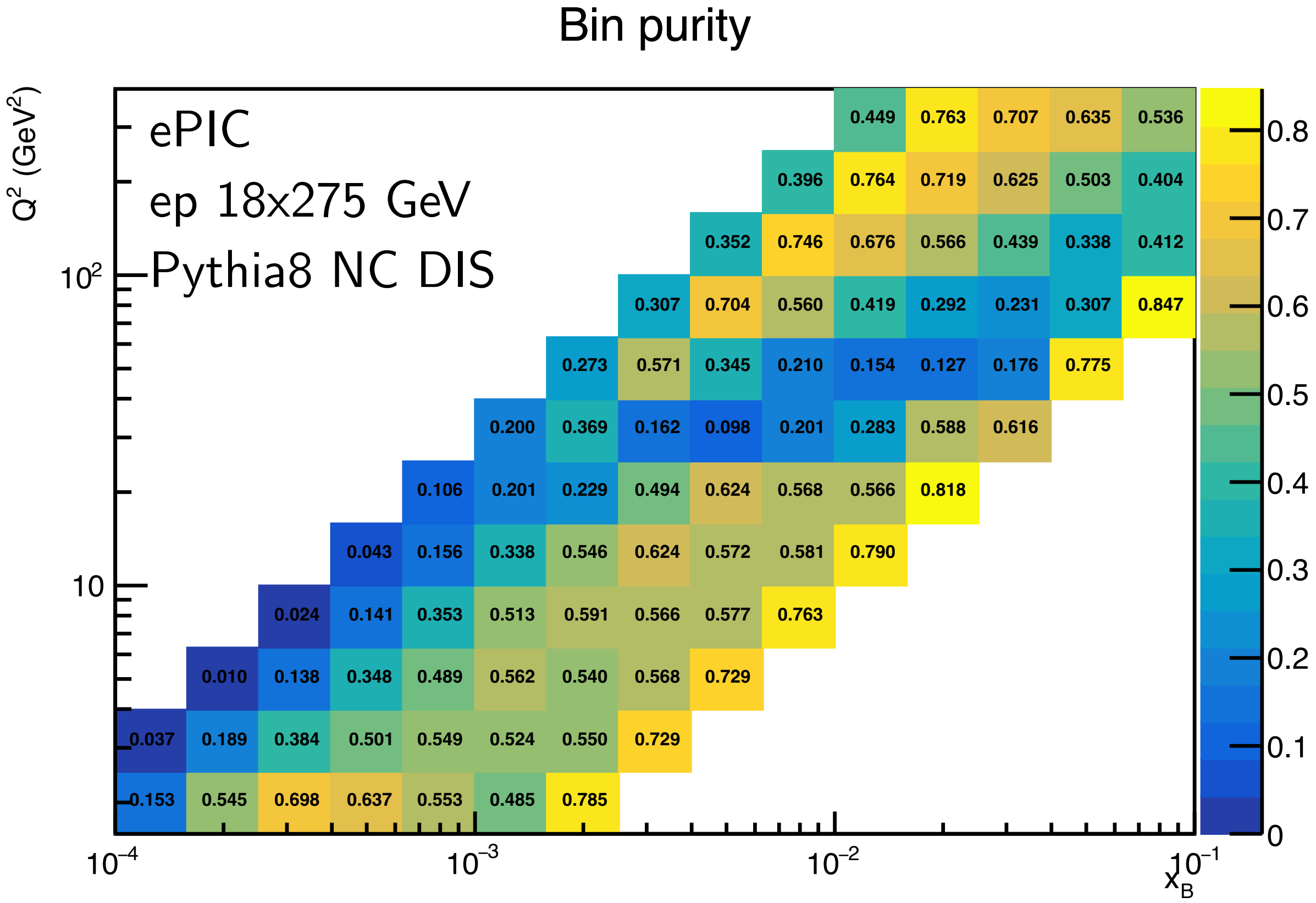


$$P = \frac{N_{gen+rec}}{N_{rec}}$$

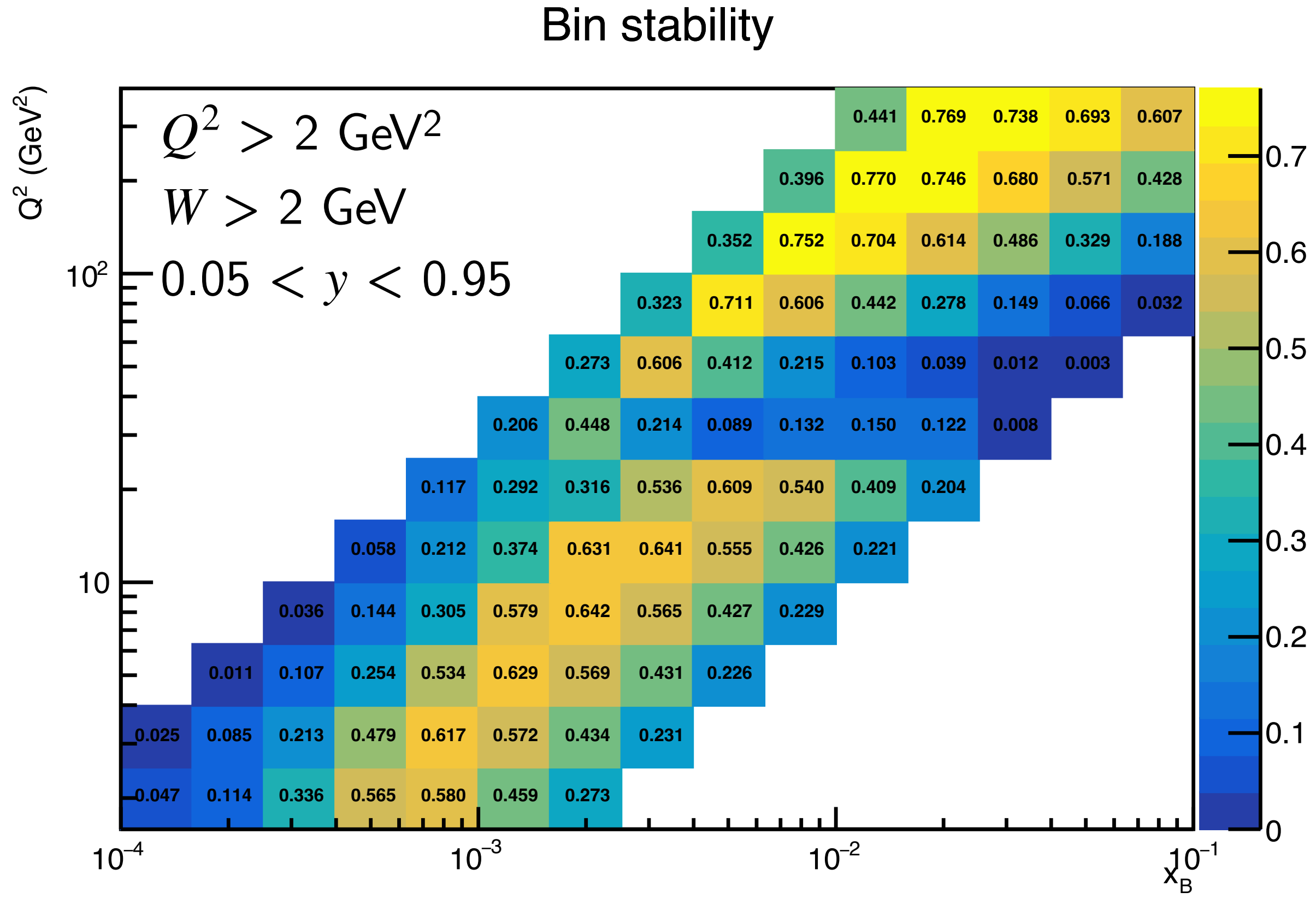
HERA  $F_L$  analyses:  
>30% required,  
>70% typical

$$S = \frac{N_{gen+rec}}{N_{gen}}$$

# Bin stability and purity (electron cluster)

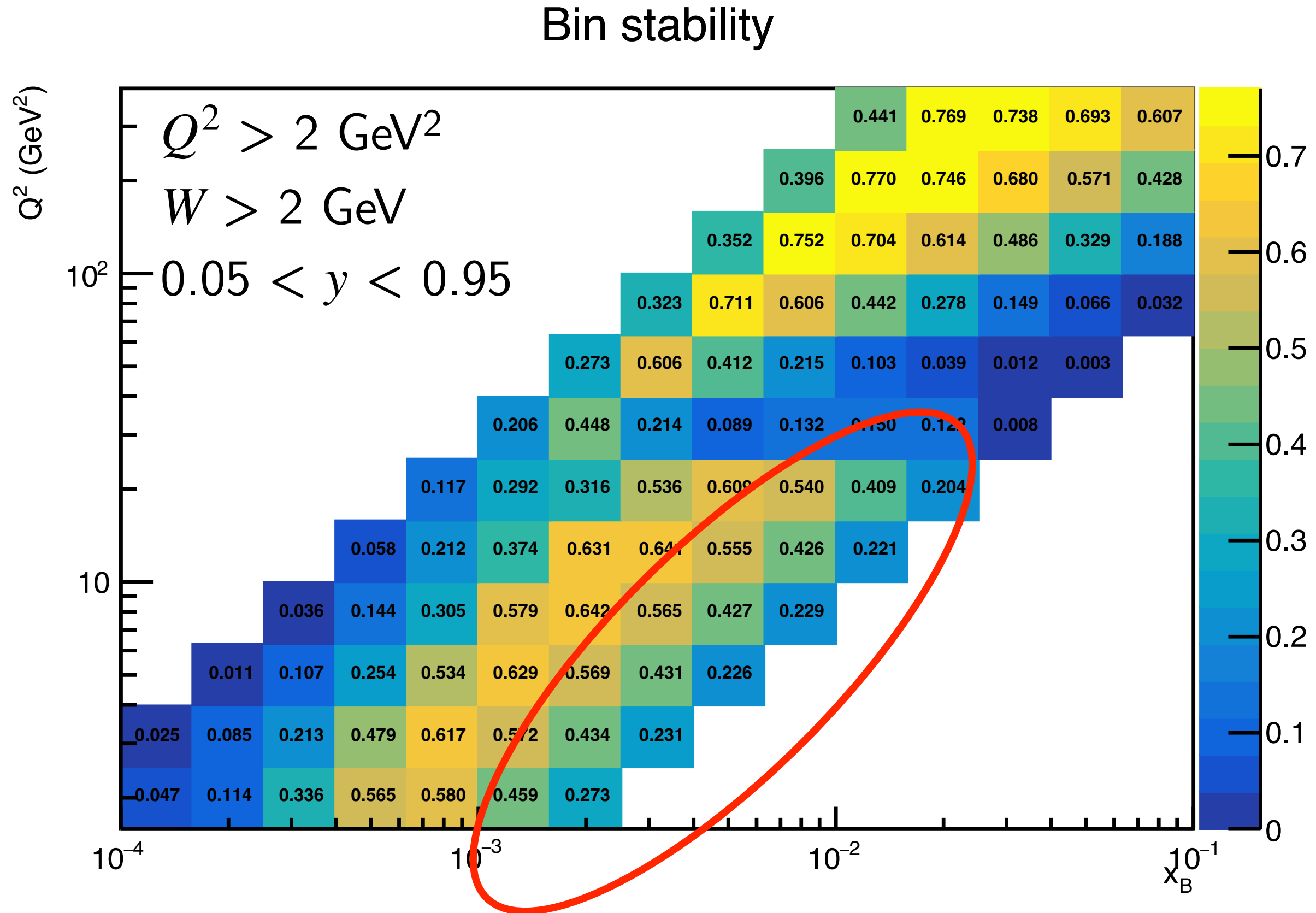
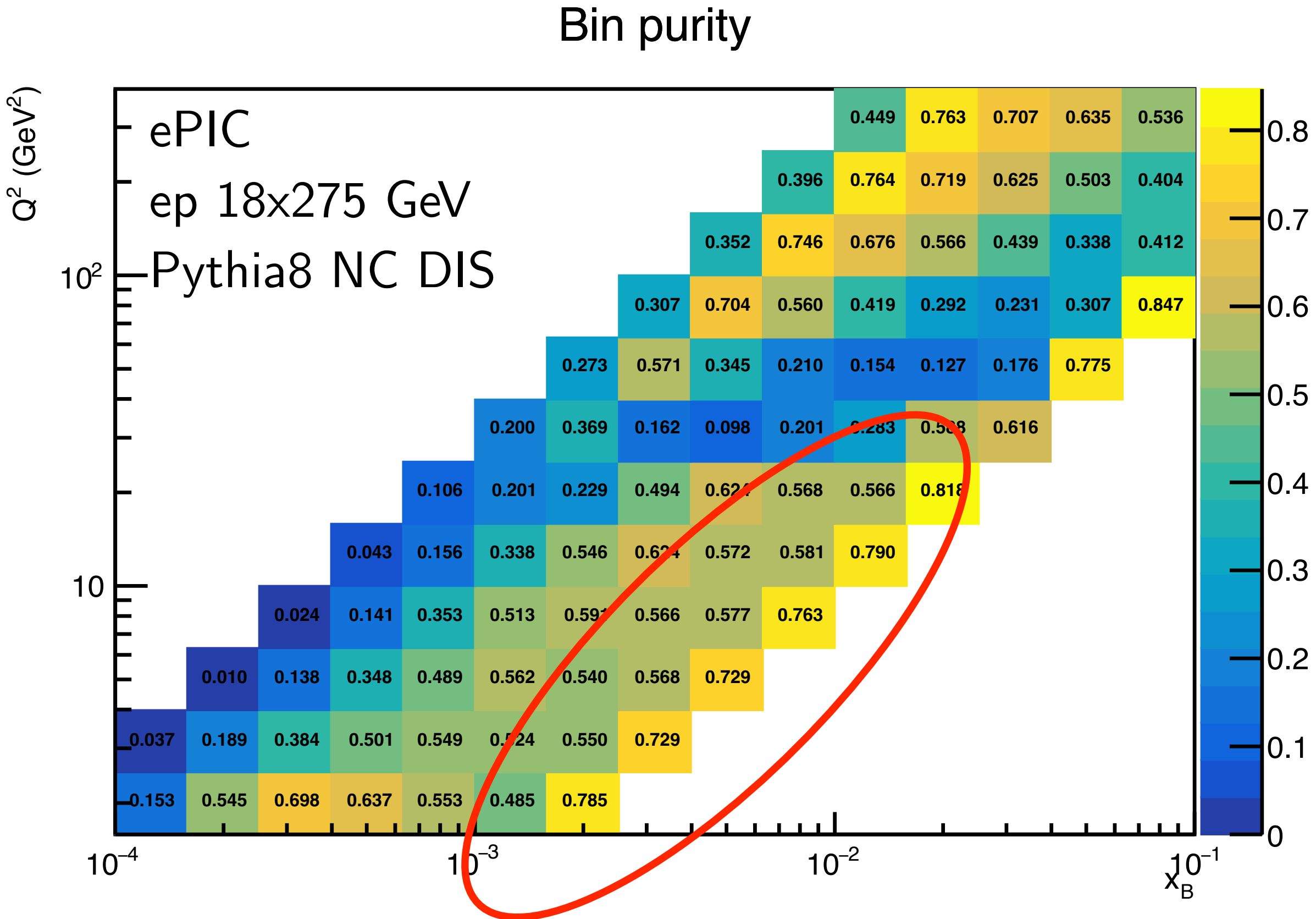


$$P = \frac{N_{gen+rec}}{N_{rec}}$$



$$S = \frac{N_{gen+rec}}{N_{gen}}$$

# Bin stability and purity (electron cluster)



$$P = \frac{N_{gen+rec}}{N_{rec}}$$

Improvement in backward ECAL region

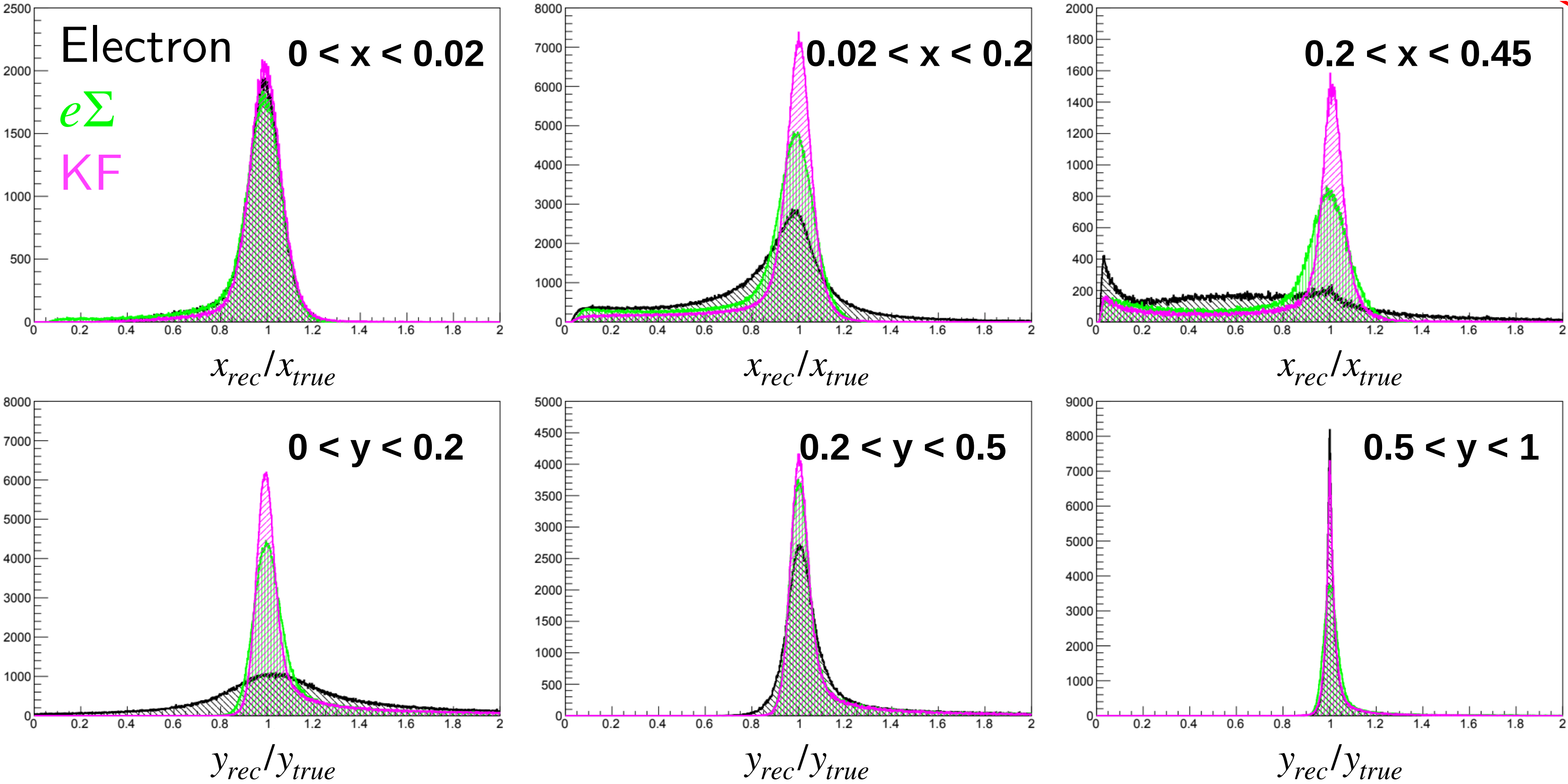
$$S = \frac{N_{gen+rec}}{N_{gen}}$$

# More advanced reconstruction methods

# More advanced reconstruction methods

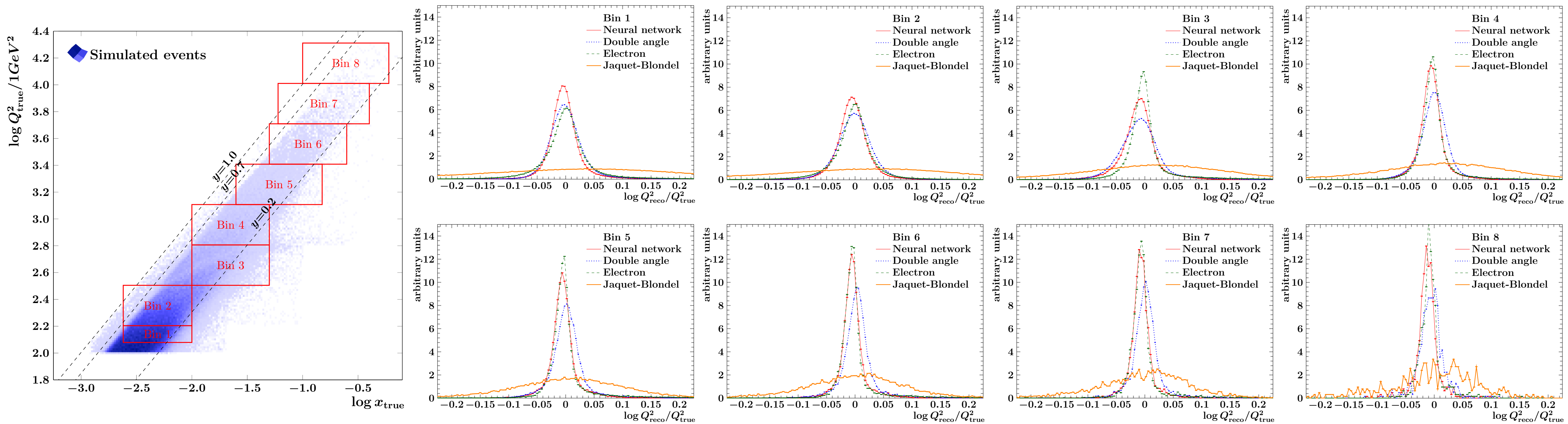
- Kinematic fitting: reconstruct  $\bar{\lambda} = \{x_B, y, E_\gamma\}$  from  $\bar{D} = \{E'_e, \theta'_e, \delta_h, p_{T,h}\}$  using likelihood function (Stephen Maple, et al.)

Proof of concept:  
Smearred  
DJANGO  
events with  
ISR



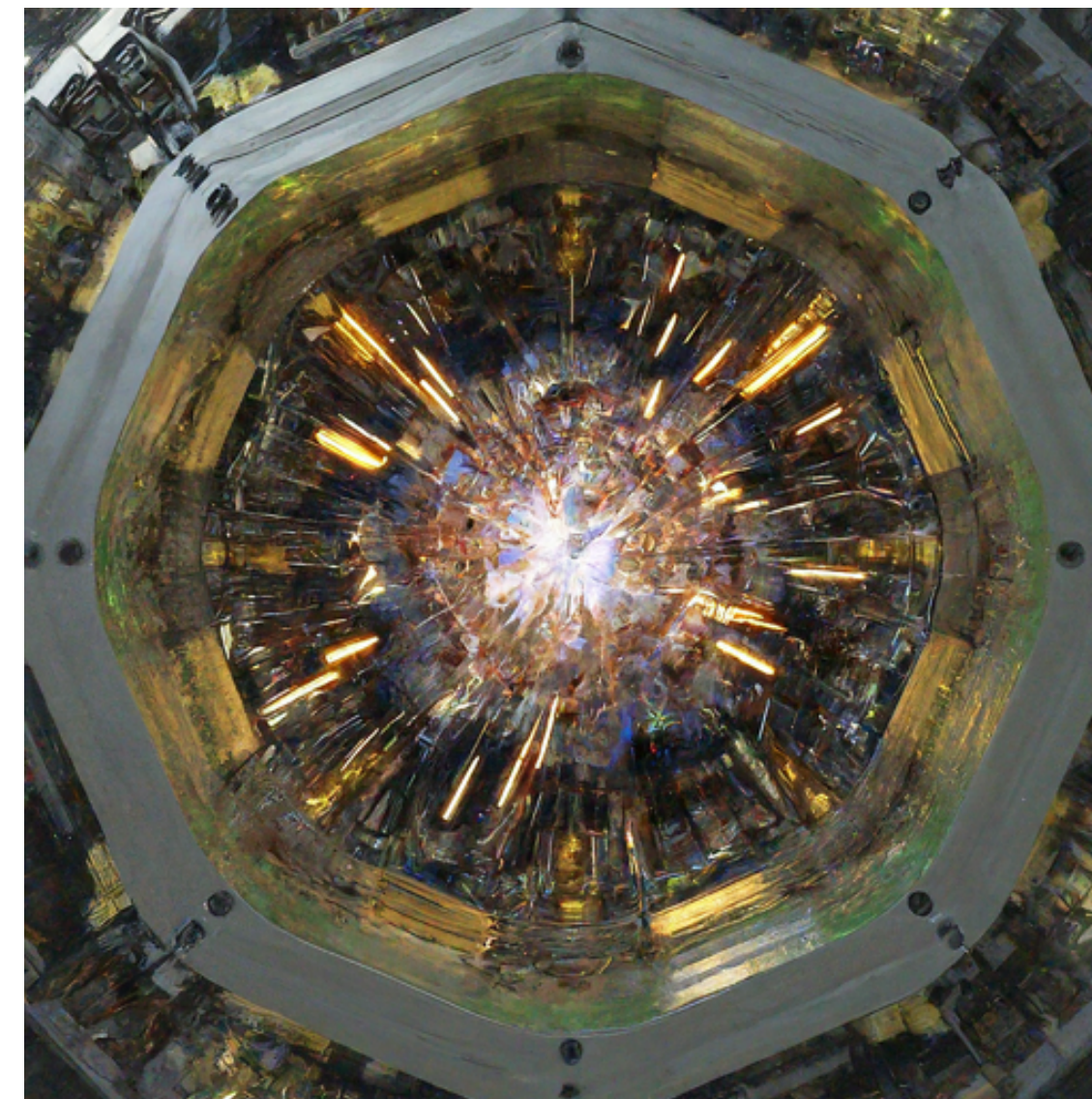
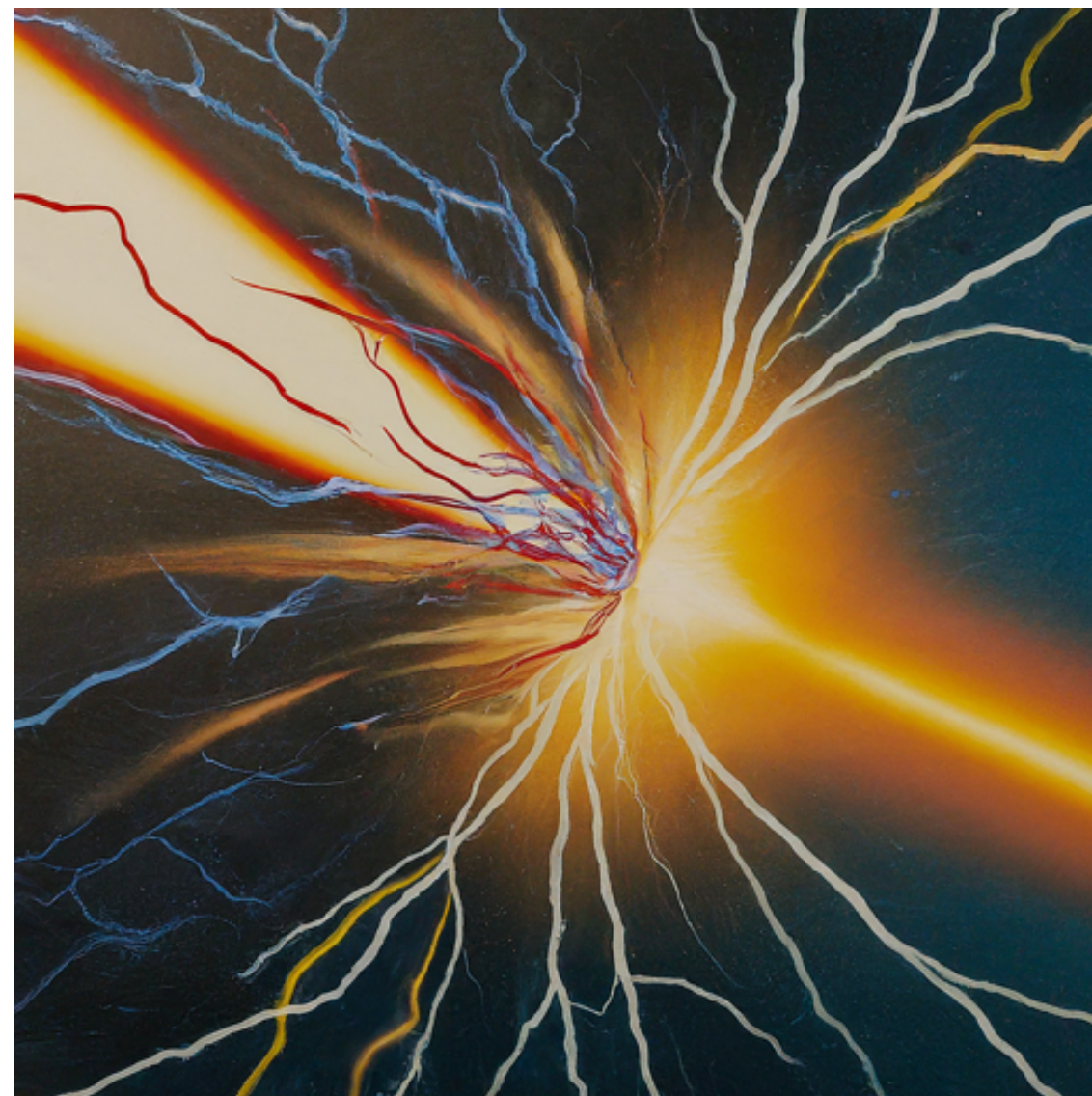
# More advanced reconstruction methods

- Kinematic fitting: reconstruct  $\bar{\lambda} = \{x_B, y, E_\gamma\}$  from  $\bar{D} = \{E'_e, \theta'_e, \delta_h, p_{T,h}\}$  using likelihood function (Stephen Maple, et al.)
- Machine learning: use simulation to train neural network ([M. Diefenthaler, A. Farhat, A. Verbytskyi and Y. Xu](#))



# More advanced reconstruction methods

- Kinematic fitting: reconstruct  $\bar{\lambda} = \{x_B, y, E_\gamma\}$  from  $\bar{D} = \{E'_e, \theta'_e, \delta_h, p_{T,h}\}$  using likelihood function (Stephen Maple, et al.)
- Machine learning: use simulation to train neural network ([M. Diefenthaler, A. Farhat, A. Verbytskyi and Y. Xu](#))
- Particle-flow: optimize combination of all detector information (Derek Anderson, et al.)



\*Images by Gemini (the AI chatbot formerly known as Bard)



# Impact of pion contamination on observables

- Pions passing all electron ID cuts give contamination  $f_{\pi/e}$
- Contamination can be corrected or treated as dilution

Cross sections

(correct contamination):

$$\left( \frac{\Delta(\sigma^{r,NC})}{\sigma^{r,NC}} \right)_{\pi^-} = \Delta f_{\pi/e}$$

$$\approx 0.1 \times f_{\pi/e}$$

# Impact of pion contamination on observables

- Pions passing all electron ID cuts give contamination  $f_{\pi/e}$
- Contamination can be corrected or treated as dilution

Cross sections

(correct contamination):

$$\left( \frac{\Delta(\sigma^{r,NC})}{\sigma^{r,NC}} \right)_{\pi^-} = \Delta f_{\pi/e}$$

$$\approx 0.1 \times f_{\pi/e}$$

Asymmetries

(treat as dilution factor):

$$\left( \frac{\sigma_{A^e}}{A^e} \right)_{\pi^-} = \sqrt{(\Delta f_{\pi/e})^2 + \left( f_{\pi/e} \frac{|A^\pi| + \Delta A^\pi}{A^e} \right)^2}$$

$$\approx 0.1 \times f_{\pi/e} - 1 \times f_{\pi/e}$$

# Impact of pion contamination on observables

- Pions passing all electron ID cuts give contamination  $f_{\pi/e}$
- Contamination can be corrected or treated as dilution

Cross sections

(correct contamination):

$$\left( \frac{\Delta(\sigma^{r,NC})}{\sigma^{r,NC}} \right)_{\pi^-} = \Delta f_{\pi/e}$$

$$\approx 0.1 \times f_{\pi/e}$$

Asymmetries

(treat as dilution factor):

$$\left( \frac{\sigma_{A^e}}{A^e} \right)_{\pi^-} = \sqrt{(\Delta f_{\pi/e})^2 + \left( f_{\pi/e} \frac{|A^\pi| + \Delta A^\pi}{A^e} \right)^2}$$

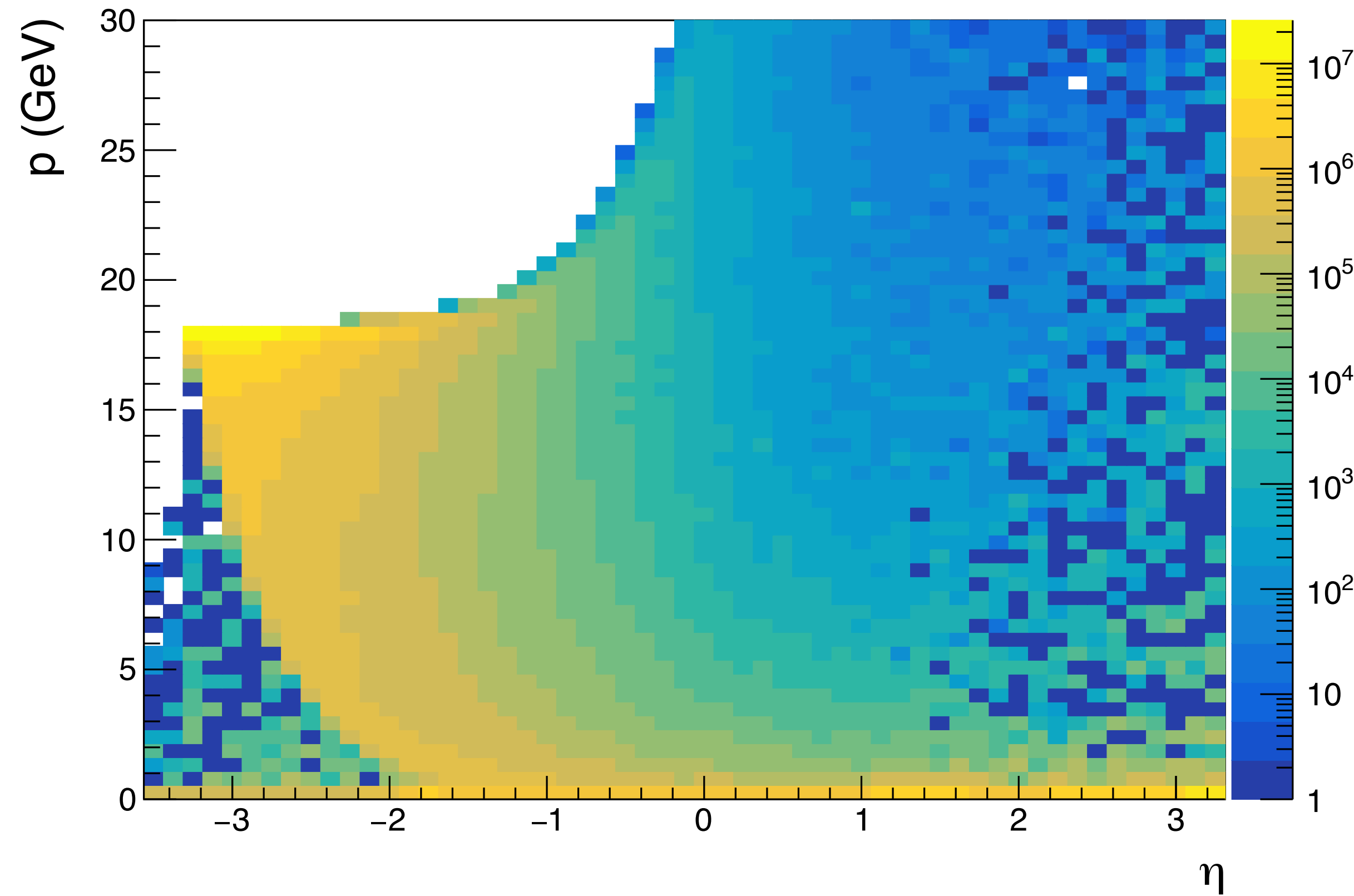
$$\approx 0.1 \times f_{\pi/e} - 1 \times f_{\pi/e}$$

Large  $A^e$ ,  
nonzero  $|A^\pi| < A^e$

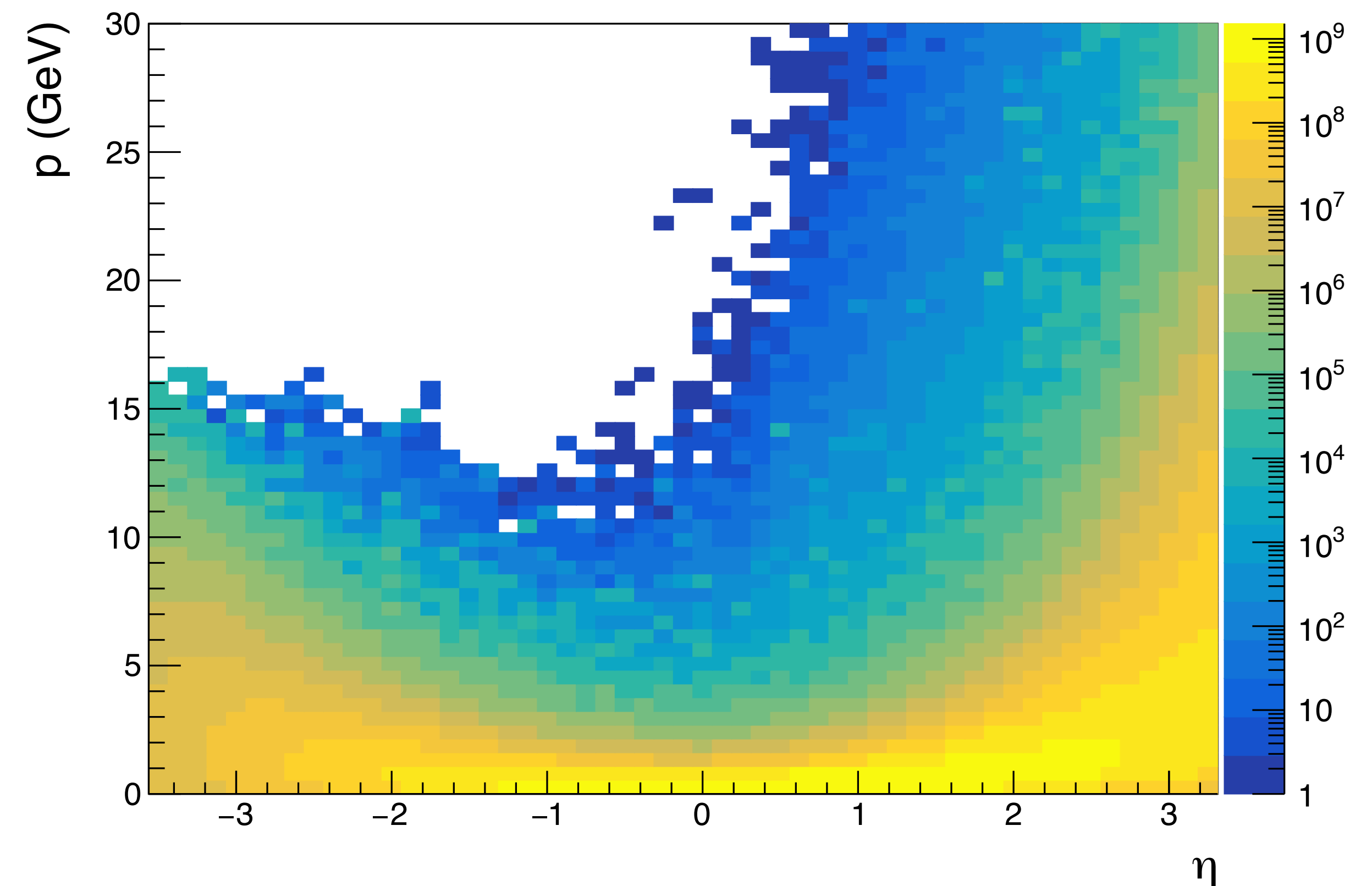
Small  $A^e$ ,  
 $|A^\pi| \approx 0$

# Electron to pion ratios

$e^-$  DIS



$\pi^-$  DIS + PHP

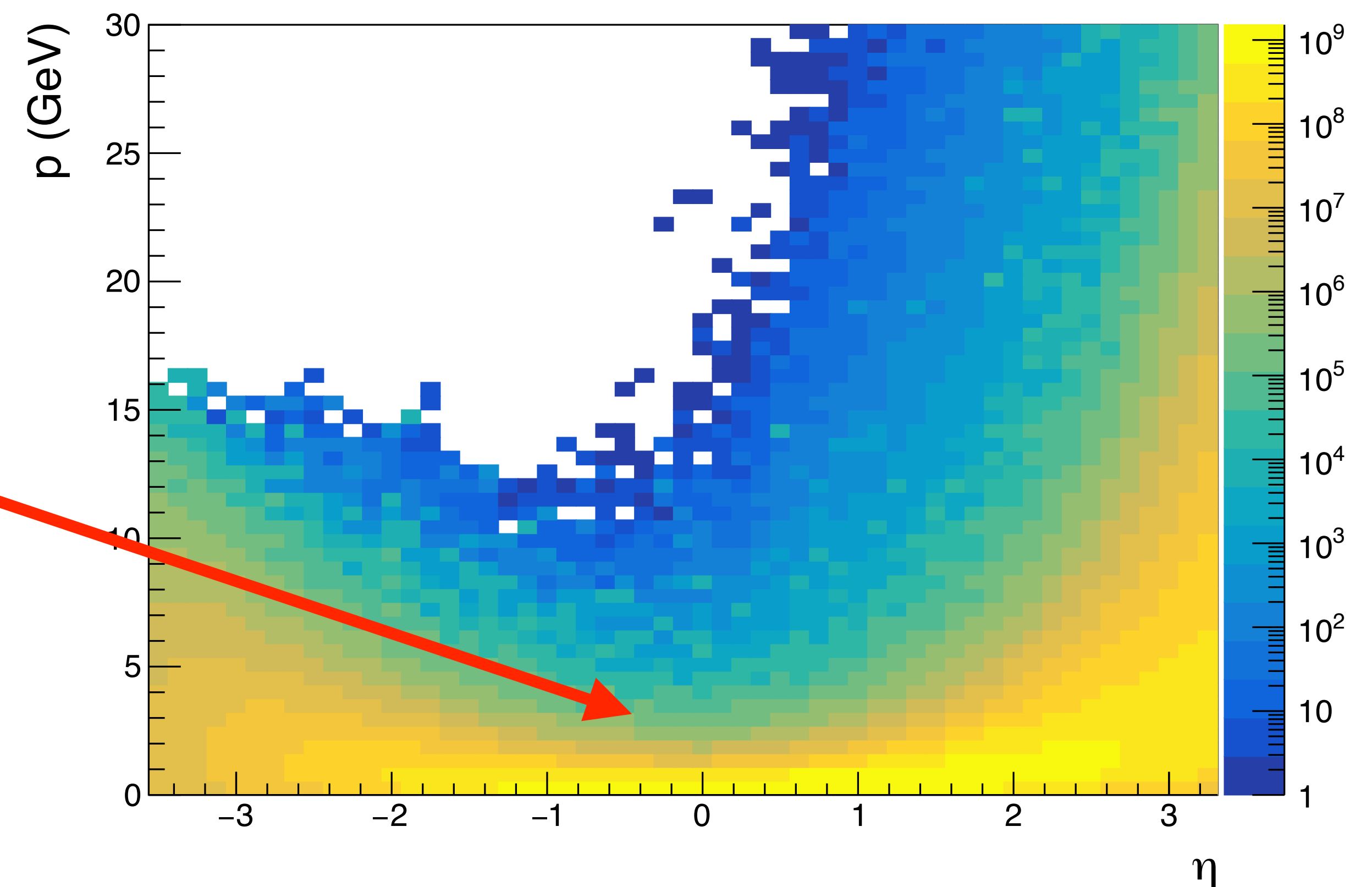
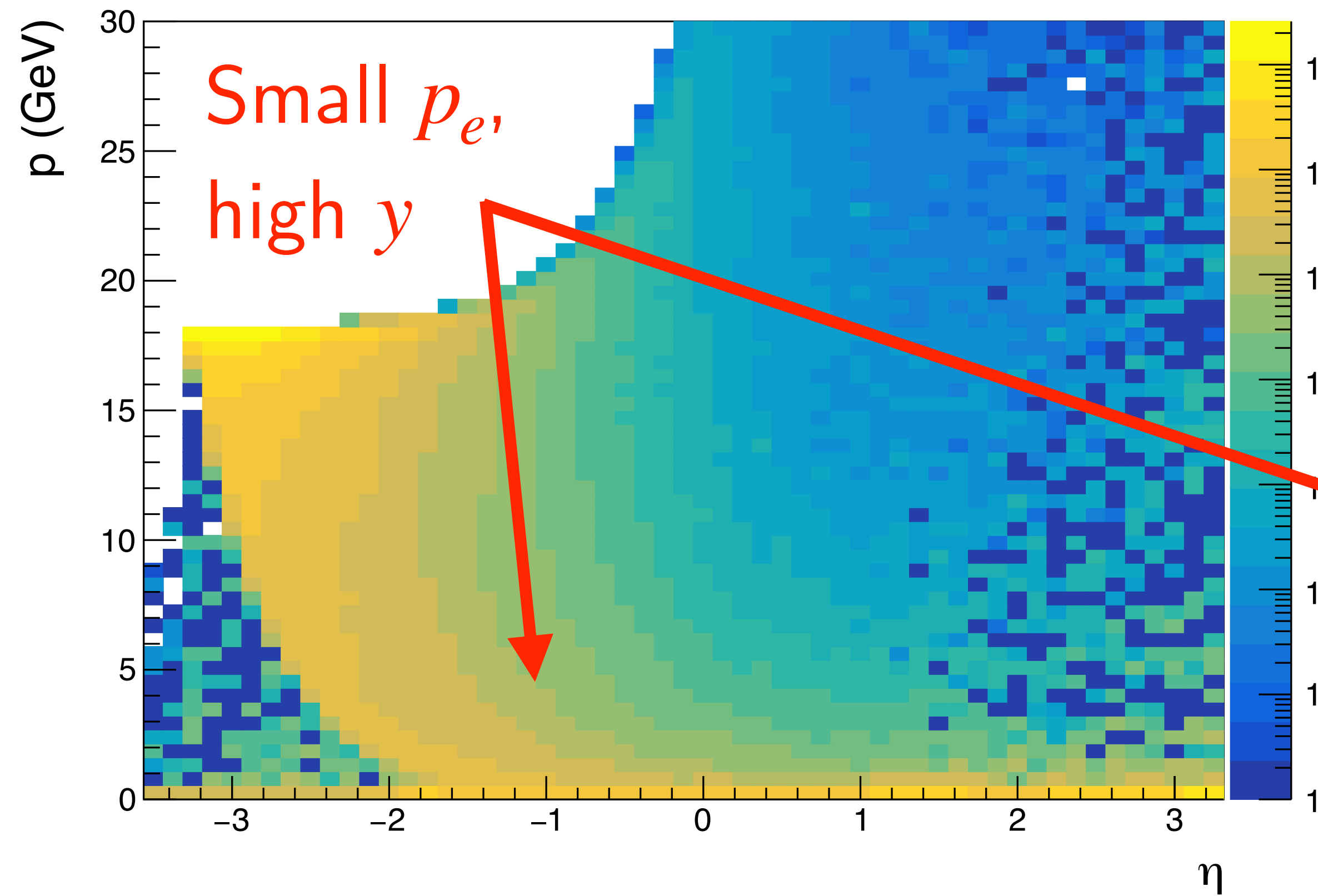


- Signal  $e^-$  from DJANGO DIS
- Background  $\pi^-$  from DJANGO DIS, Pythia6 photoproduction ( $Q^2 < 2 \text{ GeV}^2$ )

# Electron to pion ratios

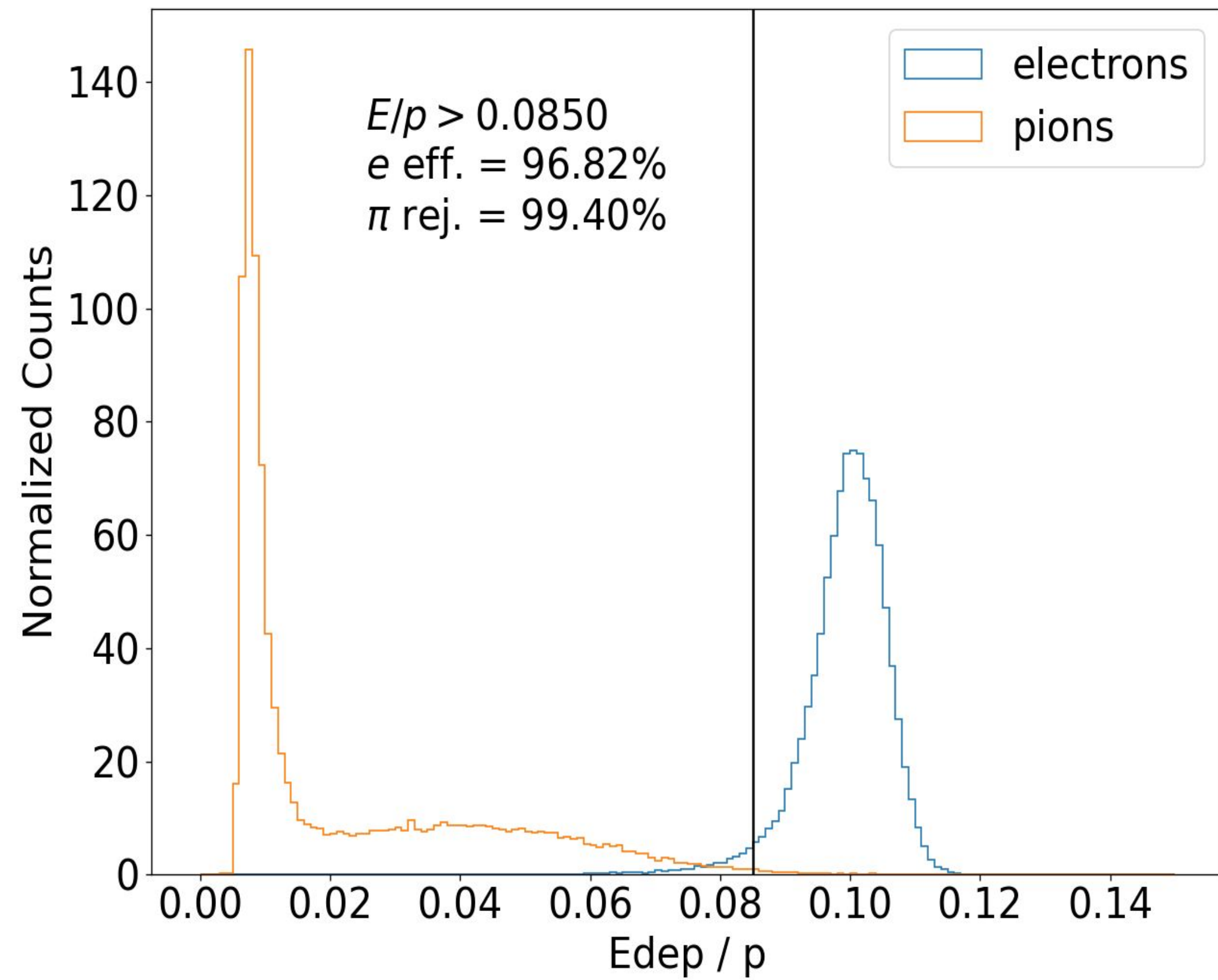
$e^-$  DIS

$\pi^-$  DIS + PHP



- Signal  $e^-$  from DJANGO DIS
- Background  $\pi^-$  from DJANGO DIS, Pythia6 photoproduction ( $Q^2 < 2 \text{ GeV}^2$ )

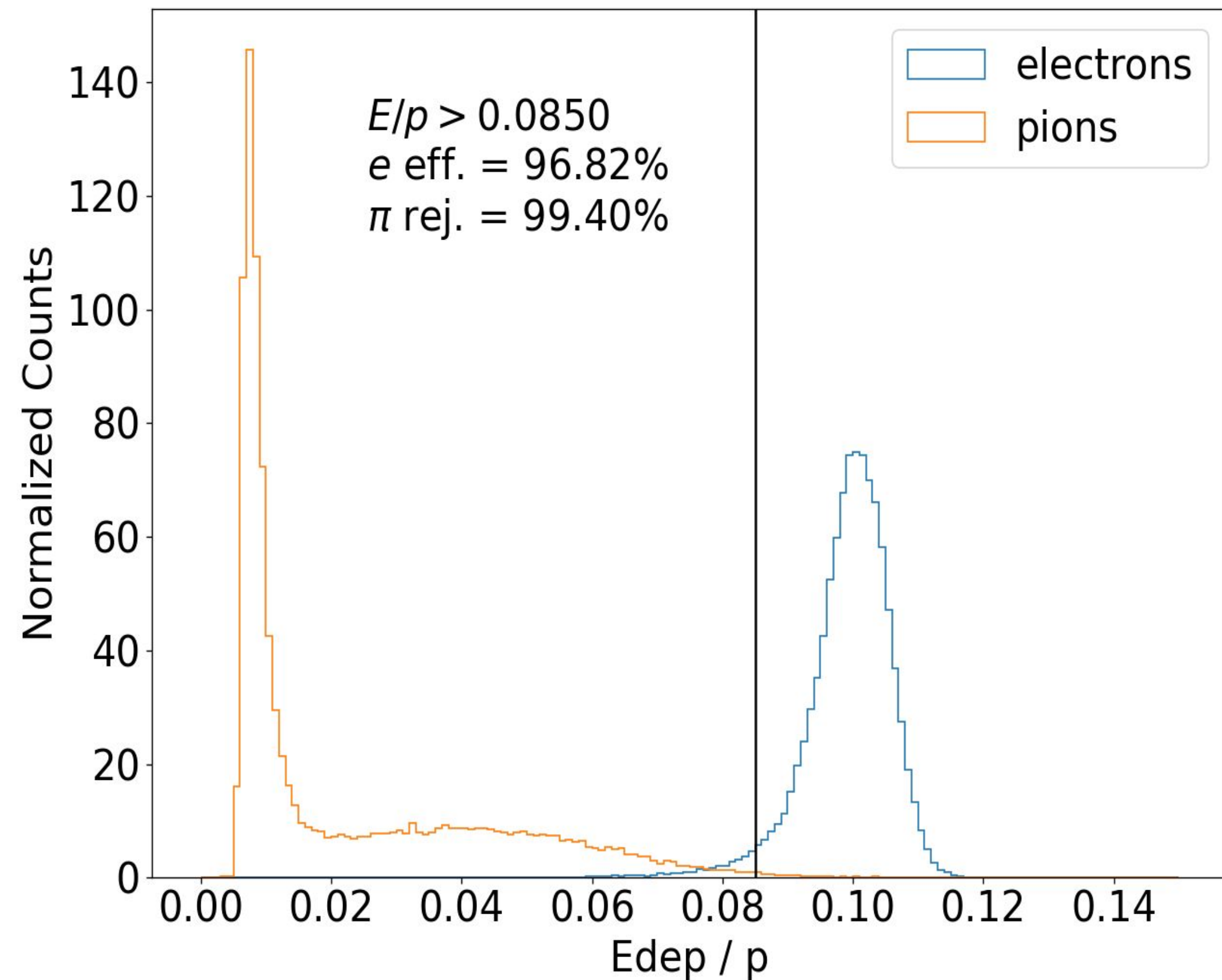
# Pion suppression cuts



Detector:

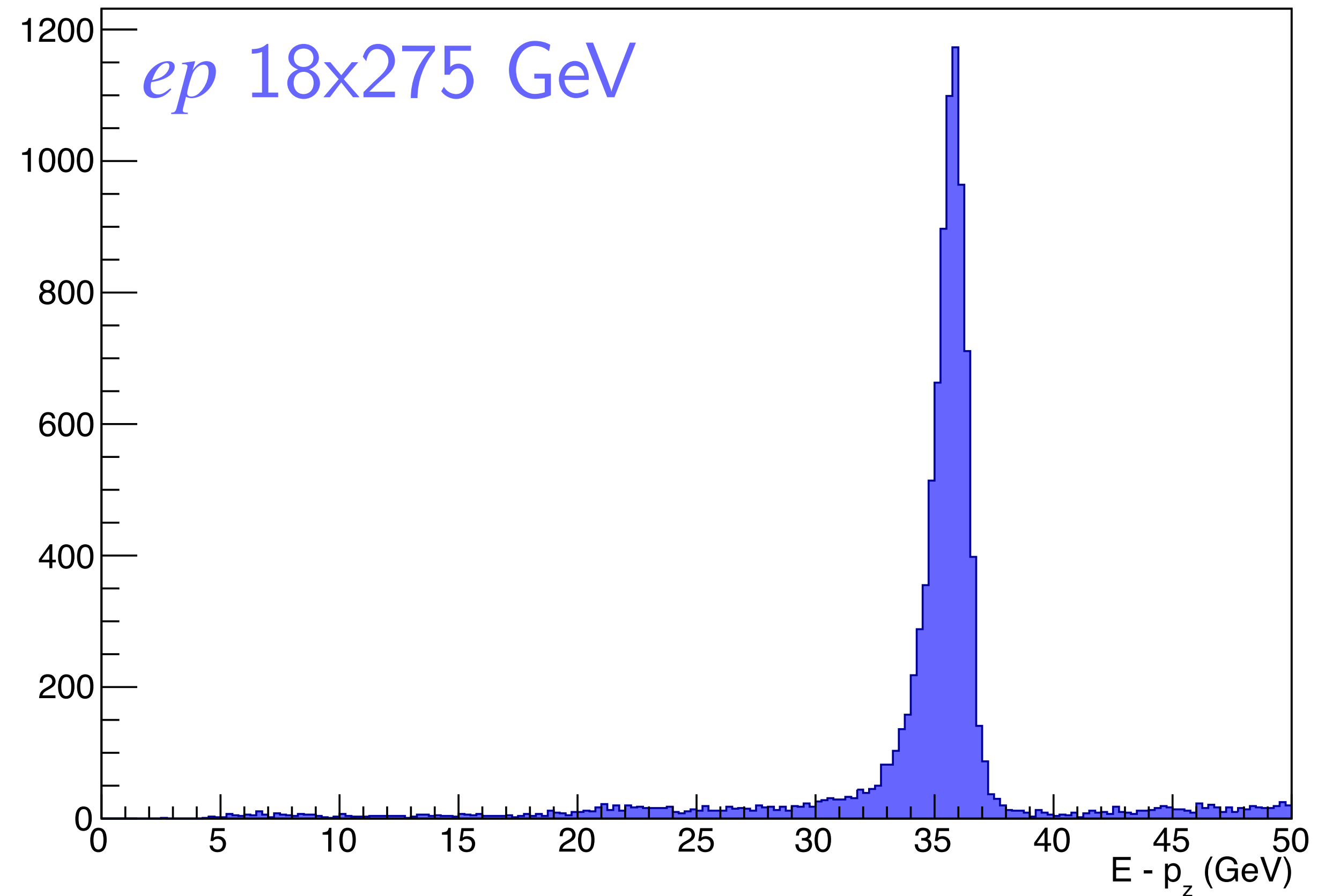
- Electrons deposit most/all energy in ECAL

# Pion suppression cuts



Detector:

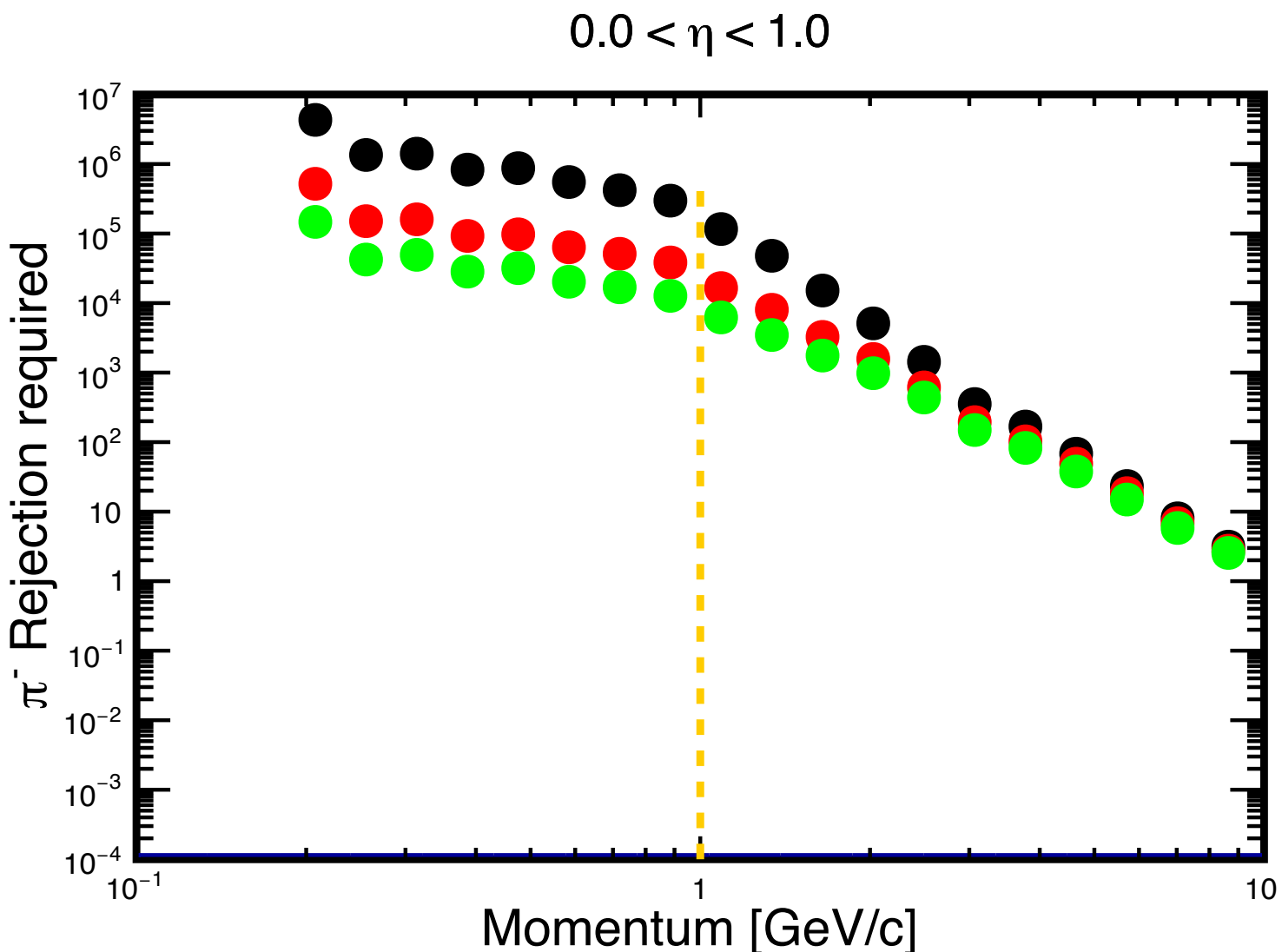
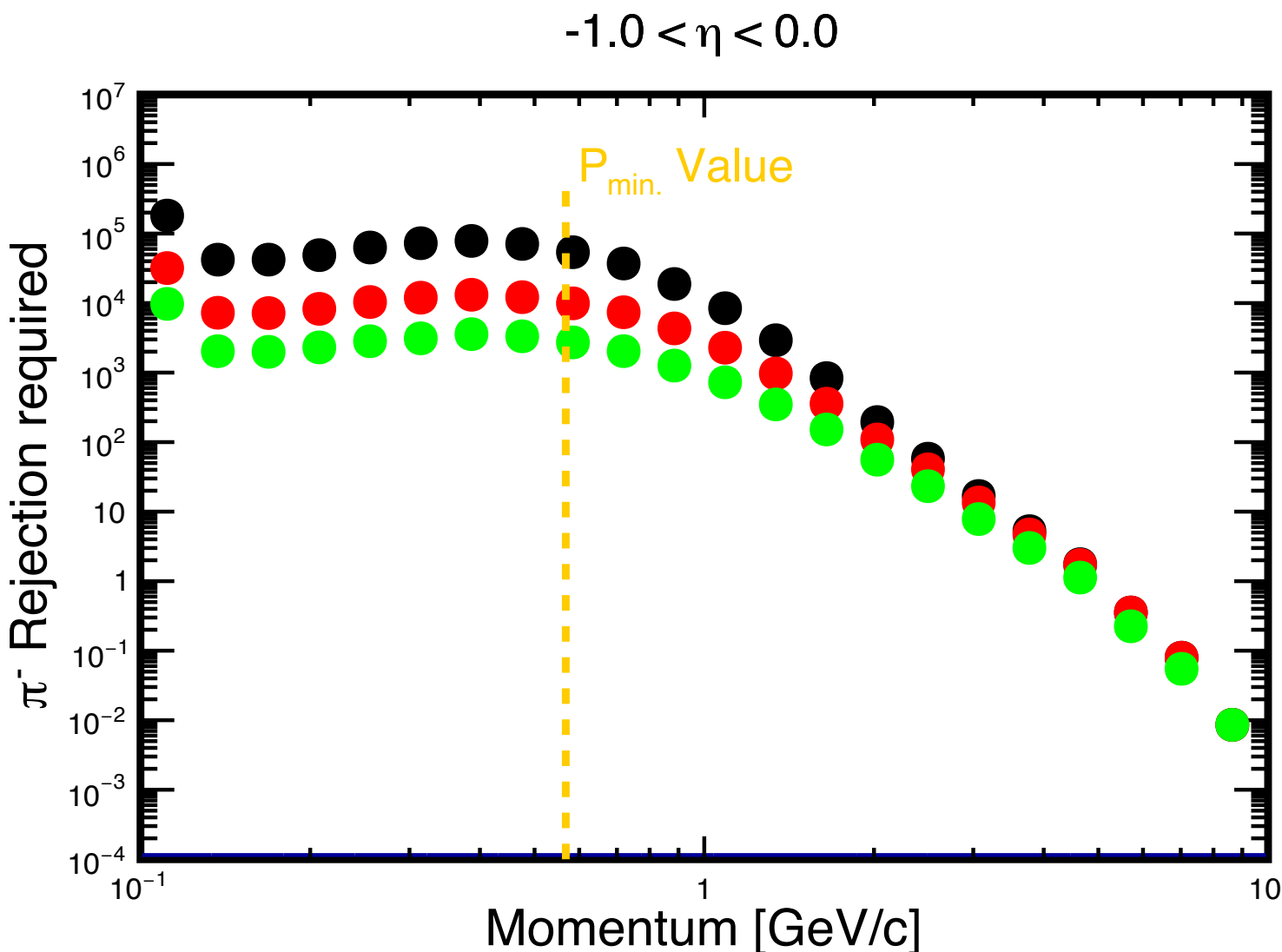
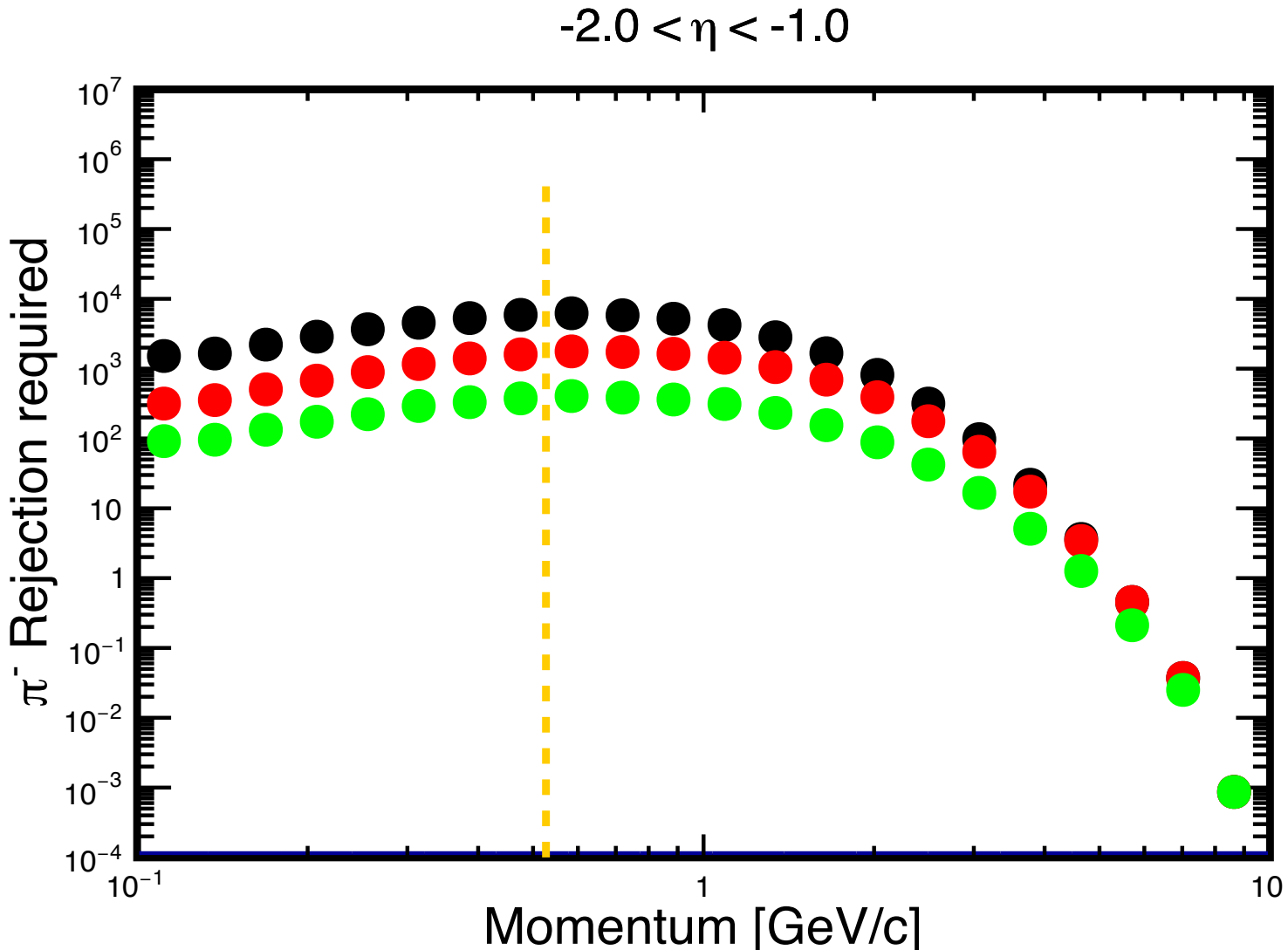
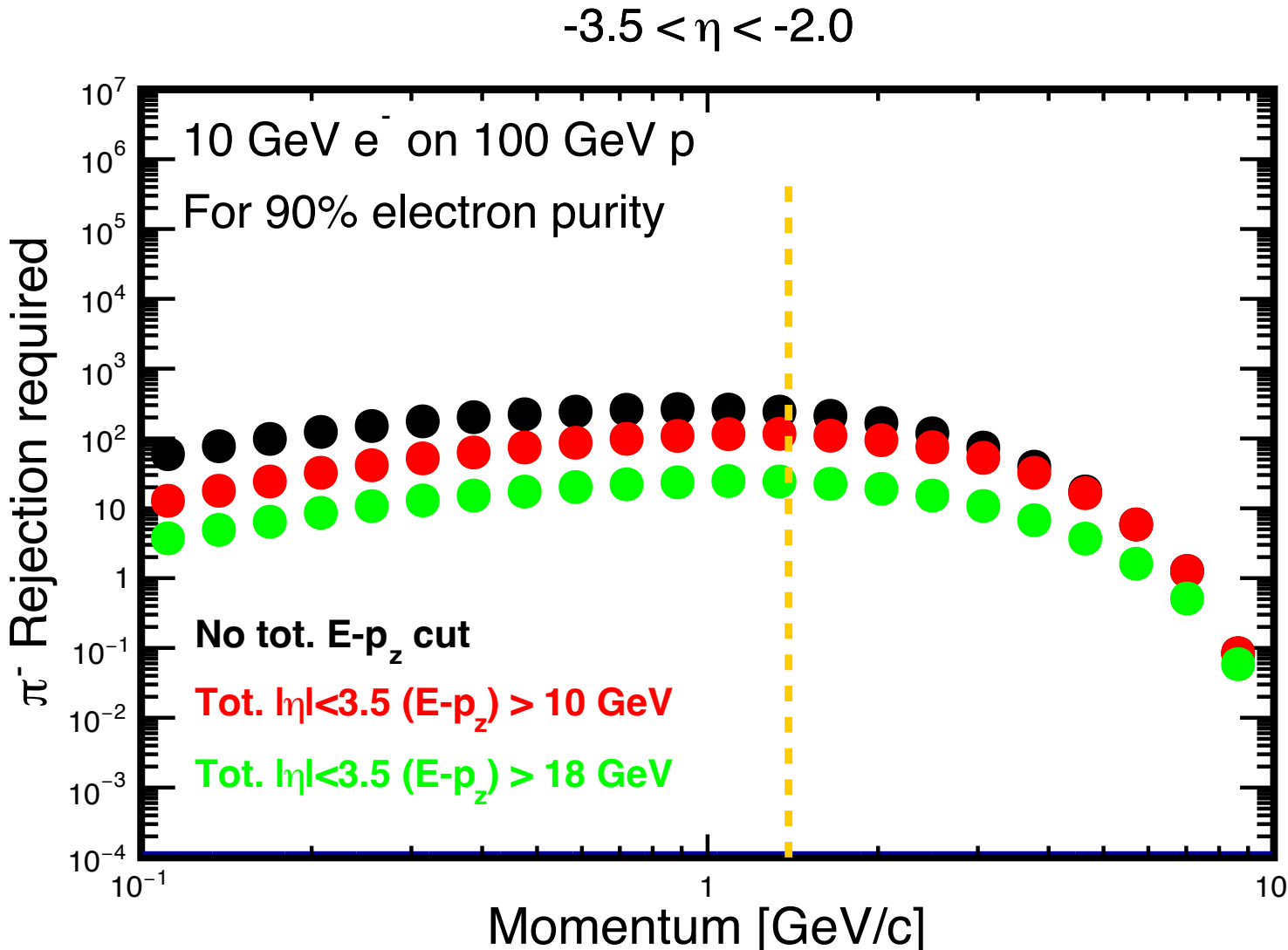
- Electrons deposit most/all energy in ECAL



Kinematic:

- If electron lost down beampipe,  $\Sigma_h(E - p_z) < 2E_e$
- Significant reduction in required  $E/p$  suppression

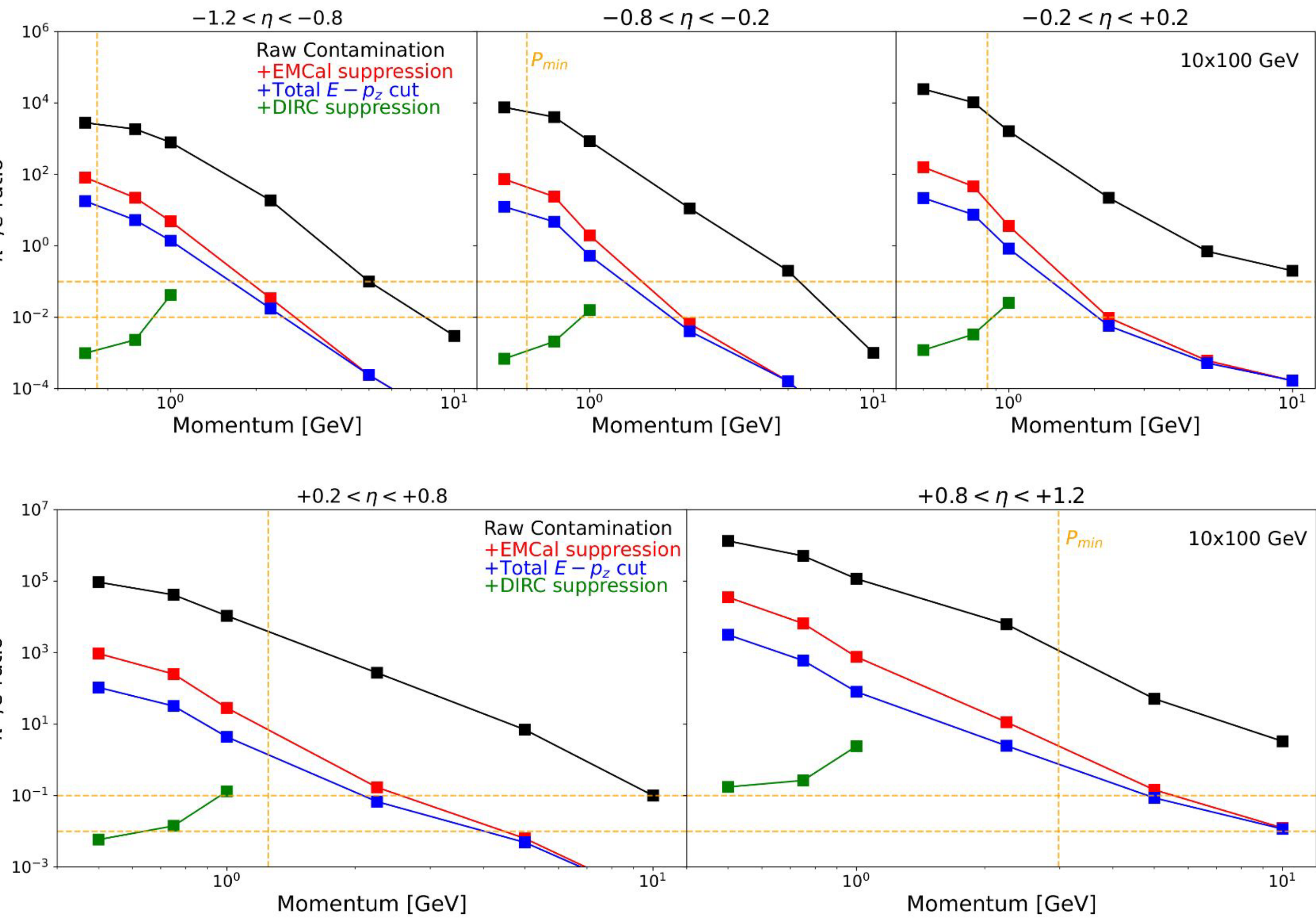
# Required suppression for 90% purity



- $E - p_z$  cut reduces required suppression by up to 20x
- Electron ID depends on how well ePIC reconstructs *hadronic* final state
- Barrel critical region due to large raw  $\pi^-/e^-$  ratio

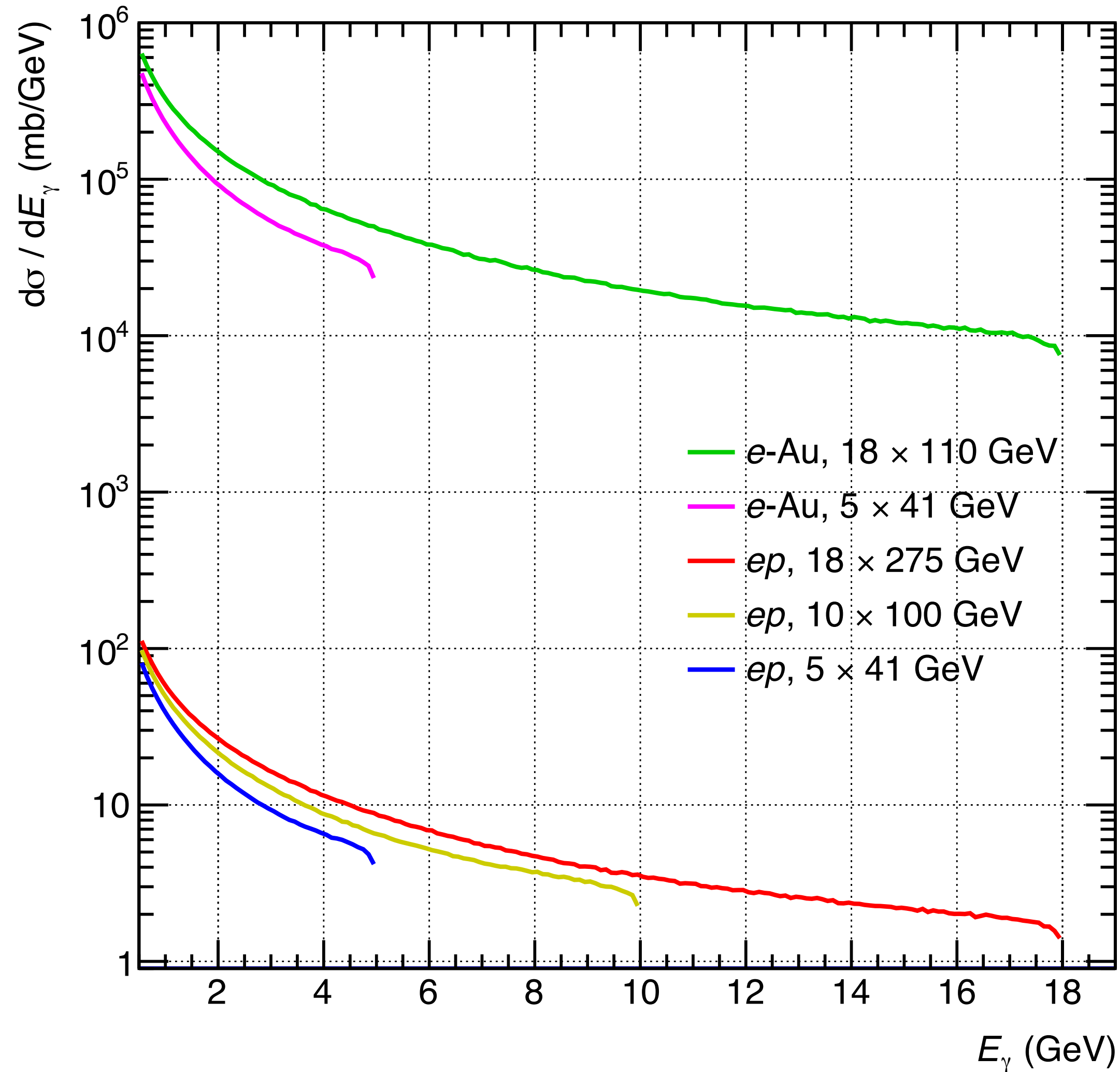


# Pion contamination in the barrel



- DIRC assists at low momentum
- Further EMCal suppression possible from shower shape

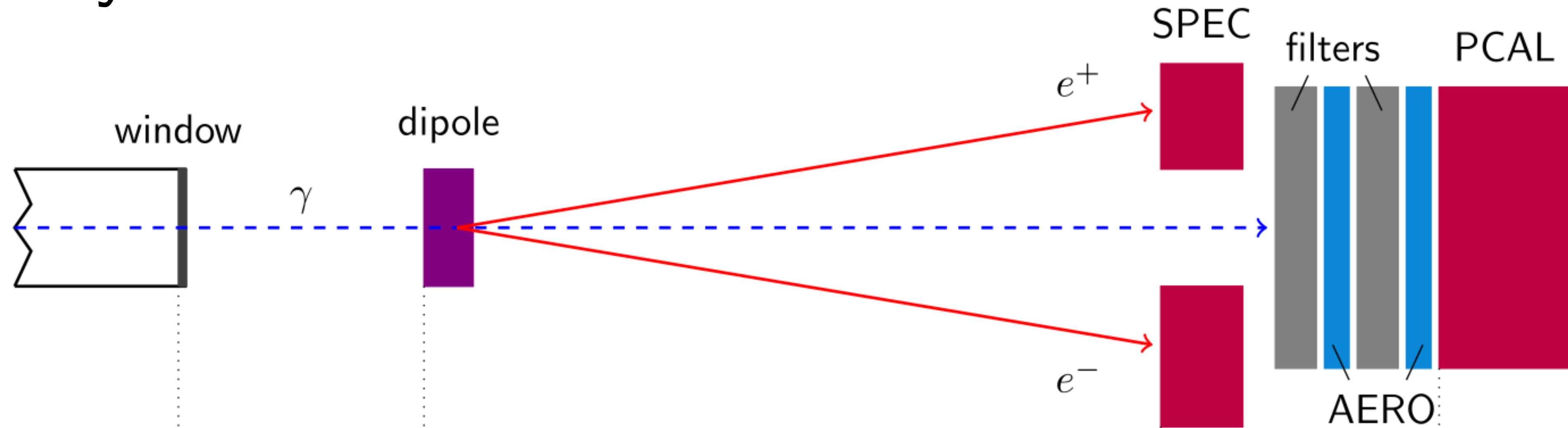
# Luminosity determination from bremsstrahlung



$$\frac{d\sigma}{dE_\gamma} = 2\alpha r_e^2 \frac{E'_e}{E_\gamma E_e} \left( \frac{E_e}{E'_e} + \frac{E'_e}{E_e} - \frac{2}{3} \right) \left( \ln \frac{4E_p E_e E'_e}{m_p m_e E_\gamma} - \frac{1}{2} \right)$$

- Large cross section driven by QED
- Significant increase in cross section with  $Z$
- Luminosity determined by photon counting

# Luminosity detectors for the EIC



- Two methods to detect bremsstrahlung photons:
  - Unconverted photons detected in preshower calorimeter
  - Converted  $e^+e^-$  pairs detected in spectrometer
- EIC goal is 1% precision:
  - Naive assumption is that uncertainty is correlated between beam configurations
  - However, relative performance of each method could depend on hadron type, beam energy

# Polarization measurements at the EIC

- Hadron polarimetry:
  - Hydrogen jet
  - p-carbon
  - Low-energy polarimeter
- Electron polarimetry:
  - Møller
  - Compton (transverse and longitudinal)
  - Mott

At RHIC, has achieved high precision  $(\delta P/P)_{sys} = 0.6\%$ ,  
but is time consuming  $(\delta P/P)_{stat} = 3.6\%$  for 8 hours

## Compton polarimetry performance

Polarimeter	Energy	Sys. Uncertainty
CERN LEP*	46 GeV	5%
HERA LPOL	27 GeV	1.6%
HERA TPOL*	27 GeV	1.9-3.5%
SLD at SLAC	45.6 GeV	0.5%
JLAB Hall A	1-6 GeV	1-3%
JLab Hall C	1.1 GeV	0.6%

\*transverse

Goal for EIC is  $\delta P/P = 1\%$  for both hadron and electron

# Theory systematics

$$\sigma(x_B, Q^2) = \frac{N - B}{\mathcal{L} \cdot \mathcal{A}} \cdot \mathcal{C} \cdot (1 + \Delta)$$

experiment

theory

- Bin-centering  $\mathcal{C}$
- Radiative corrections  $\Delta$ 
  - Recent efforts to unify QED radiative effects with QCD radiation  
[Liu, Melnitchouk, Qiu, Sato PRD 104, 094033 \(2021\)](#)
  - Electroweak radiation...?
- Traditional approach is binned *unfolding* of experiment, but event-by-event *folding* of theory becoming more feasible

# Concluding remarks

- Optimum electron, kinematic reconstruction methods differ across detector
  - Comparing kinematic bins will have different systematics
- Electron ID is critical for EIC physics
  - Asymmetry measurements limited by electron purity
  - Especially important in the barrel region, where pion background is largest
- High-precision polarimetry critical to polarized asymmetry measurements
- Absolute measurements require precise luminosity

Backup

# Definitions of reconstruction methods

Electron

$$y = 1 - \frac{E'_e}{2E_e}(1 - \cos \theta_e)$$

$$Q^2 = 2E_e E'_e (1 + \cos \theta_e)$$

Jacquet-Blondel

$$y = \frac{\delta_h}{2E_e}$$

$$Q^2 = \frac{p_{T,h}^2}{1 - y}$$

Double-angle

$$y = \frac{\sin \theta_e (1 - \cos \gamma_h)}{\sin \gamma_h + \sin \theta_e - \sin(\gamma_h + \theta_e)}$$

$$Q^2 = 4E_e^2 \frac{\sin \gamma_h (1 + \cos \theta_e)}{\sin \gamma_h + \sin \theta_e - \sin(\gamma_h + \theta_e)}$$